Characterizing the Atmospheric Mn Cycle and Its Impact on Terrestrial Biogeochemistry

Louis Lu[1, 2], Longlei Li[1], Sagar Rathod[3], Peter Hess[4], Carmen Martínez[5], Nicole Fernandez[1], Christine Goodale[6], Janice Thies[5], Michelle Wong[7], Maria Alaimo[16], Paulo Artaxo[8], Francisco Barraza[9], Africa Barreto[10], David Beddows[11], Shankarararman Chellam[12], Ying Chen[13], Patrick Chuang[14], David Cohen[15], Gaetano Dongarrà[16], Cassandra Gaston[17], Darío Gómez[18], Yasser Morera-Gómez[19], Hannele Hakola[20], Jenny Hand[21], Roy Harrison[11, 22], Phillip Hopke[23], Christoph Hueglin[24], Yuan-wen Kuang[25], Katriina Kyllonen[20], Fabrice Lambert[26, 27], Willy Maenhaut[28], Randall Martin[29], Adina Paytan[13], Joseph Prospero[17], Yenny González[10, 30], Sergio Rodriguez[10, 31], Patricia Smichowski[18], Daniela Varrica[16], Brenna Walsh[29], Crystal Weagle[29], Yi-hua Xiao[24], and Natalie Mahowald[1]

[1]Department of Earth and Atmospheric Sciences, Cornell University, Ithaca, NY, USA, [2]Now at: Nicholas School of the Environment, Duke University, Durham, NC, USA, [3]La Follette School of Public Affairs, University of Wisconsin, WI, Madison, USA, [4]Biological and Environmental Engineering, Cornell University, Ithaca, NY, USA, [5]School of Integrative Plant Sciences, Cornell University, Ithaca, NY, USA, [6]Department of Ecology and Evolutionary Biology, Cornell University, Ithaca, NY, USA, [7]Department of Ecology and Evolutionary Biology, Yale University, New Haven, CT 065118, [8]Instituto de Fisica,Universidade de Sao Paulo, 05508-090, Sao Paulo, SP, Brazil, [9]Saw Science, Invercargill, New Zealand, [10]Izana Atmospheric Research Centre AEMET, Joint Research Unit to CSIC "Climate and Composition of the Atmosphere", La Marina 20, planta 6,38001, Santa Cruz de Tenerife, Spain, [11]School of Geography, Earth and Environmental Sciences, University of Birmingham, Edgbaston, Birmingham B15 2TT, United Kingdom, [12]Department of Civil & Environmental Engineering, Texas A&M University, College Station, TX 77843-3136, USA, [13]Institute of Marine Sciences, University of California, Santa Cruz, CA, USA, [14]Earth & Planetary Sciences Department, University of California, Santa Cruz, CA, 95064 , USA, [15]Australian Nuclear Science and Technology Organisation, Lucas Heights, NSW, Australia, [16]Dip. Scienze della Terra e del Mare, University of Palermo, Italy, [17]Rosenstiel School of Marine and Atmospheric Science, University of Miami, Miami, FL, 33149, USA, [18]Comisión Nacional de Energía Atómica, Universidad de Buenos Aires, Argentina, [19] Universidad de Navarra, Instituto de Biodiversidad y Medioambiente BIOMA, Irunlarrea 1, 31008, Pamplona, España, [20]Finnish Meteorological Institute, Helsinki, Finland, [21]Cooperative Institute for Research in the Atmosphere, Colorado State University, Fort Collins, CO, USA, [22]Department of Environmental Sciences, Faculty of Meteorology, Environment and Arid Land Agriculture, King Abdulaziz University, Jeddah, Saudi Arabia, [23]Department of Chemical and Biomolecular Engineering, Clarkson University, Potsdam, NY, USA, [24]Swiss Federal Laboratories for Materials Science and Technology (EMPA), CH-8600 Duebendorf, Switzerland, [25]Key Laboratory of Vegetation Restoration and Management of Degraded Ecosystems,South China Botanical Garden, Chinese Academy of Sciences, Guangzhou 510650, China, [26]Geography Institute, Pontificia Universidad Católica de Chile, Santiago, 7820436, Chile, [27]Center for Climate and Resilience Research, University of Chile, Santiago, Chile, [28]Department of Chemistry, Ghent University, Gent, Belgium, Institute for Nuclear Sciences,

University of Gent, Belgium, [29]Energy, Environmental and Chemical Engineering, Washington University, St. Louis, MO, USA, [30]CIMEL Electronique, Paris, 75011, France, [31]Instituto de Productos Naturales y Agrobiología IPNA CSIC, La Laguna, Canary Islands, Spain.

Corresponding author: Louis Lu (pl230@duke.edu)

†Additional author notes should be indicated with symbols (current addresses, for example).

Key Points:

- We modelled the atmospheric manganese (Mn) cycle from emission to deposition and compared our aerosol model to existing observations based on our compilation.
- Anthropogenic activity contributes to approximately one-third of global atmospheric Mn, shortening the soil Mn turnover time by 1 to 2 orders of magnitude.
- Mn correlates with topsoil carbon (C) in temperate and (sub)tropical forests, along with N deposition and other climatic factors.

Abstract

Manganese (Mn) is a key cofactor in enzymes responsible for lignin decay (mainly Mn peroxidase), regulating the rate of litter degradation and carbon (C) turnover in temperate and boreal forest biomes.While soil Mn is mainly derived from bedrock, atmospheric Mn could also contribute to soil Mn cycling, especially within the surficial horizon, with implications for soil C cycling. However, quantification of the atmospheric Mn cycle, which comprises emissions from natural (desert dust, sea salts, volcanoes, primary biogenic particles, and wildfires) and anthropogenic sources (e.g. industrialization and land-use change due to agriculture) transport, and deposition into the terrestrial and marine ecosystem, remains uncertain. Here, we use compiled emission datasets for each identified source to model and quantify the atmospheric Mn cycle with observational constraints. We estimated global emissions of atmospheric Mn in aerosols (<10 μm in aerodynamic diameter) to be 1500 Gg Mn yr^{-1}. Approximately 32% of the emissions come from anthropogenic sources. Deposition of the anthropogenic Mn shortened soil Mn "pseudo" turnover times in surficial soils about 1-m depth (ranging from 1,000 to over 10,000,000 years) by 1-2 orders of magnitude in industrialized regions. Such anthropogenic Mn inputs boosted the Mn-to-N ratio of the atmospheric deposition in non-desert dominated regions (between 5×10-5 and 0.02) across industrialized areas, but still lower than soil Mn-to-N ratio by 1-3 orders of magnitude. Correlation analysis revealed a negative relationship between Mn deposition and topsoil C density across temperate and (sub)tropical forests, illuminating the role of Mn deposition in these ecosystems.

1 Introduction

As an essential trace element and micronutrient, manganese (Mn) has been identified to be closely related to soil carbon (C) turnover because of its role of regulating soil organic matter (SOM) decomposition by enhancing the activity of lignin-decay enzymes (mainly Mn peroxidase, MnP) and hence the oxidative decomposition of lignin (Berg et al., 2007; Hofrichter, 2002). Mn limitation and the associated fungal community change from N deposition have been proposed as an explanation for the suppressing effect of long-term atmospheric nitrogen (N) deposition on SOM decomposition (Moore et al., 2021; Whalen et al., 2018).

Studies have assessed the relationship between Mn and soil C turnover using various indicators including Mn concentration in litter, rate or extent of decomposition of litter (Berg et al., 2007, 2010; Berg 2000; Davey et al., 2007; Trum et al., 2015), soil Mn and total C concentrations (Stendahl et al., 2017), MnP enzymatic activity, and fungal community structures (Kranabetter et al., 2021; Moore et al., 2021; Whalen et al., 2018). However, no previous study has examined the impact of atmospheric Mn deposition on soil C turnover, nor has such a relationship been quantified on a global scale. In fact, atmospheric deposition has been identified as a major source of metal(loid) accumulation, including Mn, in surficial soil layers (He & Walling, 1997; Kaste et al., 2003; Puchelt et al., 1993; Wang et al., 2022) where most fresh organic matter accumulates, underlining the need to characterize atmospheric Mn deposition for more advanced understanding of soil C turnover.

While atmospheric Mn deposition has not been extensively investigated, studies have shown the importance of atmospheric deposition of iron (Fe), which has similar biogeochemical properties as Mn (Canfield et al., 2005), for understanding marine biogeochemistry (Mahowald et al., 2009). In oceans, atmospheric deposition of Fe could be a stronger source of Fe than the

weathering of rock (Canfield et al., 2005); Mn deposition could act similarly as a non-negligible source of ocean Mn which could have significant ecological relevance such as co-limitation of phytoplankton growth with Fe (Browning et al., 2021; Mahowald et al., 2018). More recently, Mn catalysis of organic C polymerization reactions was proposed to result in organic carbon preservation and storage in marine sediments (Moore et al., 2023). Together, these studies show that atmospheric Mn deposition could play an important role in the global Mn cycle and is likely linked to functions carried out by Mn in both terrestrial and marine ecosystems.

There is a variety of natural sources of Mn, such as desert dust (the single dominant source), sea salts, volcanoes, wildfires, and primary biogenic particles (Nriagu, 1989; Pacyna & Pacyna, 2001). In addition to natural sources of atmospheric Mn deposition, humans can perturb the global atmospheric Mn cycle by significantly altering desert dust and adding anthropogenic emission sources, such as combustion (Mahowald et al., 2018). Anthropogenic aerosols have the potential to inducing a more rapid impact on ecosystems because of their higher solubility owing to their smaller particle size, higher carbon content, chemical and surface associations, and reactions that occur during the process of combustion (Desboeufs et al., 2005; Jang et al., 2007; Sedwick et al., 2007; Voutsa & Samara, 2002) compared to natural aerosols.

While global budgets for many metals have been estimated previously, the spatial distribution of Mn deposition and the overlap with N deposition are unknown. Nriagu (1989) made the first attempt to estimate Mn emissions to the atmosphere. Nriagu (1989) and Pacyna & Pacyna (2001) identified desert dust as the single dominant source, and estimated the contribution of anthropogenic sources to be approximately 11%. Mahowald et al. (2018) estimated that anthropogenic emissions represented ~1% of the total aerosol Mn sources. Uncertainties are high due to the lack of observational data, and so far, there have been no detailed spatially explicit studies of the atmospheric Mn cycle. Therefore, a better estimation of the Mn source budget (both natural and anthropogenic) along with its spatial distribution is necessary for understanding the global Mn cycle and its influence on terrestrial ecosystems.

In this study, we conducted the first 3-d modeling of the emission, atmospheric transport, and deposition of atmospheric Mn from multiple sources including natural and anthropogenic dust, sea salts, volcanoes, wildfires, and primary biogenic particles. We compile emission datasets for each source and soil Mn concentration measurements for the emission modeling and model calibration, respectively. We synthesized observational and modeling evidence to characterize the spatial distribution of atmospheric Mn and to assess the anthropogenic perturbation to it in both $PM_{2.5}$ and PM_{10} size fractions (atmospheric particulate matter, PM, <2.5 and 10 μm in aerodynamic diameter, respectively), which are used as common measures for aerosols in the atmosphere and included in the model (Mahowald et al., 2014; Ryder et al., 2019). To understand the importance of atmospheric deposition as a flux in the Mn cycle and as a source of Mn addition to soils in terrestrial ecosystems, we interpreted soil Mn “pseudo” turnover times and Mn-to-N ratios in deposition as well as the relationship between Mn deposition and C density in topsoil.

2 Materials and Methods

2.1 Soil Mn Observations and Interpolation

We compiled soil observational data collected from 94 studies found using the Thomson Web of Science Core Collection on March 20, 2022 and the soil characterization database provided in National Cooperative Soil Survey (NCSS). There are 2068 individual data points in total, reporting worldwide Mn concentrations in surface soils based on several extraction and digestion methods (Data Set S1). A standard approach is HNO3 + HCl acid digestion as outlined by the U.S. Department of Agriculture (USDA) and Natural Resources Conservation Service (NRCS) (Soil Survey Staff, 2011). If detailed geographical coordinates were not explicitly provided, we assigned the observation of the nearest latitude and longitude based on available information about its location. Two approaches (linear interpolation and extrapolation by soil type) were used to extrapolate the limited observational data to provide global estimates of Mn distributions in soils.

2.1.1 Linear Interpolation

Our first approach was to linearly interpolate observed soil Mn concentrations according to their geographical coordinates and extrapolate them on a global map (Figure 1a) using inverse distance method in GRIDDATA function on board with Interactive Data Language. Because directly extrapolating all available soil Mn data is a straightforward, the constructed soil map from linear interpolation was a fairly good representation of observations ($r = 0.66$; Figure 1a). Nonetheless, the correlation was weaker than one would expect for linear interpolation due to the model grid resolution and the fact that many observational sites clustered in a single grid. Because ice and glaciers were not considered as soil, and available observations near the poles were lacking, Mn concentrations in glaciated areas (mostly Greenland and Antarctica) were masked and assigned a minimum value.

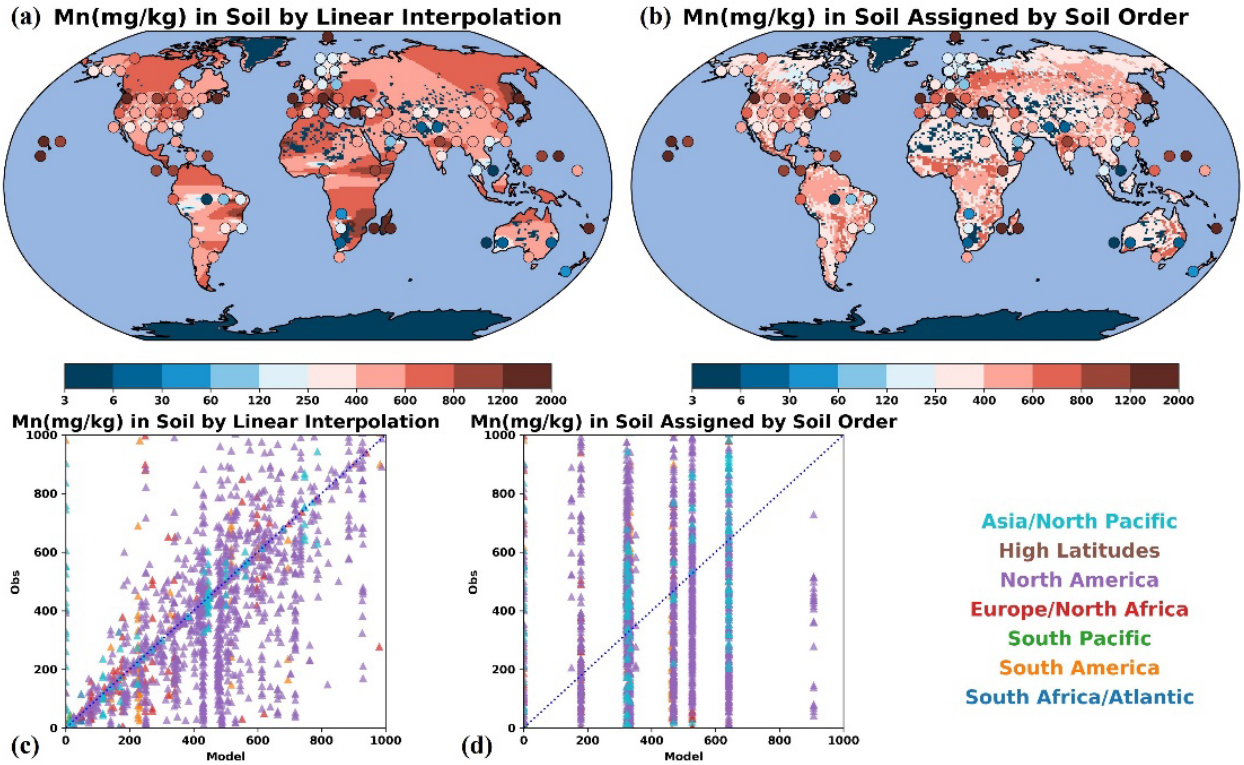

Figure 1. (a) Map of estimated global soil Mn concentration constructed from linear interpolation and (b) by soil-order extrapolation. The base map is compared to 2068 individual observational points (mg kg-1 Mn in surface soils), which are spatially averaged and plotted as circles filled with colors corresponding to their Mn concentration (Abanda et al., 2011; Alfaro et al., 2015; Alongi et al., 2004; Andruszczak E., 1975; Asawalam & Johnson, 2007; Becquer et al., 2010; Beygi & Jalali, 2018; Bibak et al., 1994; Boente et al., 2017; Bradford et al., 1996; Buccolieri et al., 2010; Burt et al., 2011; Cabrera et al., 1999; Cancela et al., 2002; Cassol et al., 2020; Chen et al., 1991; Chen et al., 1999, 2000; da Silva Costa et al., 2017; da Silva et al., 2015; Dantu, 2010a, 2010b; Darwish & Poellmann, 2015; de Souza et al., 2015; do Nascimento et al., 2018; Dolan et al., 1990; Fernandes et al., 2018; Foulds, 1993; Franklin et al., 2003; Ghaemi et al., 2015; Haynes & Swift, 1991; Hsu et al., 2016; Hua et al., 2013; Ikem et al., 2008; Imran et al., 2010; Iñigo et al., 2011; Ivezic et al., 2011; Jahiruddin et al., 2000; Joshi et al., 2017; Kassaye et al., 2012; Kloss et al., 2014; Lavado & Porcelli, 2000; Lindell et al., 2010; Ma et al., 1997; Mashi et al., 2004; McKenzie, 1957; Michopoulos et al., 2004, 2017; Mikkonen et al., 2017; Miko et al., 2003; Morales Del Mastro et al., 2015; Nalovic & Pinta, 1969; Nanzyo et al., 2002; Natali et al., 2009; Navas & Lindhorfer, 2005; Nguyen et al., 2018; Njofang et al., 2009; Nygard et al., 2012; Papadopoulos et al., 2009; Papastergios et al., 2011; Patel et al., 2015; Paye et al., 2010; Preda & Cox, 2002; Rashed, 2010; Rekasi & Filep, 2012; Richards et al., 2012; Roca et al., 2012; Roca-Perez et al., 2004, 2010; Rusjan et al., 2006; Saglam, 2017; Sako et al., 2009; Salonen & Korkka-Niemi, 2007; Sheikh-Abdullah, 2019; Sheppard et al., 2009; Skordas et al., 2013; Smeltzer et al., 1962; Stajković-Srbinović et al., 2018; Stankovic et al., 2012; Stehouwer et al., 2010; Steinnes et al., 2000; Sterckeman et al., 2006a; Sterckeman et al., 2006b;

Su & Yang, 2008; Tsikritzis et al., 2002; Tume et al., 2011; Tyler, 2004; Vance & Entry, 2000; Vejnovic et al., 2018; Wen et al., 2018; Wilcke et al., 2005; Xianmo et al., 1983; Yalcin et al., 2007; Yang et al., 2012; Yang et al., 2013; Yilmaz et al., 2003; Yu et al., 2012; Zhang et al., 2009; Zorer et al., 2009). (c) Scatter plot showing how well the linearly interpolated map represents the observations (n = 2068, r = 0.66). (d) Same as (c), except for targeting the soil-order extrapolated map. Model values equal observational values along the blue dotted diagonal (n = 2068, r = 0.08). Colors indicate the locations of studies listed in the legend. Citations of each study and details on its extraction/digestion methods are included in the supporting information (Data Set S1).

2.1.2 Extrapolation by Soil Type

In our second approach, we categorized Mn concentration observations according to their soil taxonomic classification. Using the same method as in Wong et al. (2021), we processed Mn concentration from 1574 (out of 2068) data points which provided in-situ soil classification information in either the United States Department of Agriculture (USDA), Food and Agriculture (FAO) taxonomic system, or the World Reference Base for Soil Resources (WRB) (the latter two were converted into USDA classification). A median value was assigned for each of the 12 USDA soil orders and the Mn concentration was extrapolated to the 1° × 1° USDA-NRCS Global Soil Regions map based on a reclassification of the FAO-UNESCO Soil Map of the World (Figure 1b) (Batjes, 1997). In addition to the 12 soil orders, the map also identified lands that were not covered by soils, including ice/glaciers, moving sands, rocky terrains, and water bodies, whose Mn concentration was masked and set to the minimum.

Nonetheless, because the Mn variability within soil orders were shown to be on the same level as that between soil orders (Figure S1), Mn concentration might not be well-distinguished in different soil orders. In addition, the number of available soil measurements varied greatly between different orders (Table S1) so that in cases where very few observations existed (e.g. gelisol), the median value of the soil Mn concentration would be much less representative. Our soil data inventory reflected the heterogeneous nature of the spatial distribution of the soil and its Mn content, which could not be well-represented by soil-type extrapolation. Overall, the soil-order based map did not compare as well to the in-situ soil Mn observations as the linear interpolation (Figure 1d). Therefore, the soil map and model simulations constructed using linear interpolation were primarily considered in data analysis and interpretation, with results obtained by soil-type extrapolation listed in supplementary materials and minorly concerned. Given the scarce nature of soil Mn observations, we kept the soil-type extrapolation method, as it might still be a reasonable approach to estimate and constrain soil Mn values, especially in regions lacking direct observations, such as the higher latitudes.

2.2 Atmospheric Modeling

We simulated global atmospheric Mn emissions, transport, and deposition using the Community Atmosphere Model, version 6 (CAM6), the atmospheric component of the Community Earth System Model (version 2; CESM2) developed at the National Center for Atmospheric Research (NCAR) (Hurrell et al., 2013; Liu et al., 2011), with the four-mode (Aitken, accumulation, coarse, and primary) modal aerosol model (MAM4) (Liu et al., 2016). Three out of the four modes contain dust aerosols which are modeled as eight different types of dust mineral components (Liu et al., 2011; Scanza et al., 2015; Hamilton et al., 2019; Li et al., 2021, 2022). Model simulations were conducted for four years, with the last three years (2013-2015) used for analysis (Computational and Information Systems Laboratory, 2019). We nudged the model toward MERRA2 meteorology fields (Gelaro et al., 2017).

The model simulates three-dimensional transport and wet and dry deposition for gases and particles which are internally/externally mixed within/between the modes. The dry deposition parameterization follows Petroff and Zhang (2010) as previously impletmented in CAM6 (Li et al., 2022 ; see descriptions therein for the wet deposition scheme as well). We modified the model to allow for the advection of Mn from different sources. Both natural and anthropogenic sources were determined to possess large uncertainties in strength. We used a first estimate assuming that the full uncertainty range is one order of magnitude. Therefore, we included a range of values (typically a factor of 10) for the Mn contribution from each source (Table 1). To better fit the observational data, we "tuned" the model making a particular effort to adjust anthropogenic emissions both because of their larger uncertainties compared to natural emissions and because the largest discrepancies occurred over industrialized regions (see below). The choice of the "tuning" for each source was done using a trial-and-error method using observational evidence. In addition, we report our best estimates and assume a large uncertainty: in most cases at least one order of magnitude because of the limited data as previous studies suggest (e.g. Nriagu, 1989; Mahowald et al., 2018).

Table 1

Mn Emission Factor (composition) in Sources and Atmospheric Mn Budgets Based on Simulations from the Community Atmosphere Model (CAM) (v6)

Source	Mn composition	Composition citation	Global source Mn (Gg yr^{-1}) [ranges] (% fine)	Global source Mn (Gg yr^{-1}) from reference*
Desert dust	0.1-5479 mg kg^{-1}	This study	950 [290-4800] (1.7)	42-400[a] 900[b]
Agricultural dust	0.1-5479 mg kg^{-1}	This study	390 [120-1900] (1.7)	
Sea-salt aerosols	95 μg kg^{-1}	Nriagu (1989)	0.26 [0.13-1.3] (3.3)	0.02-1.7[a]
Volcanoes	12E-4 Mn/S	Nriagu (1989)	3.9 [2.0-20] (47)	4.2-80[b]
Primary biogenic particles	60 mg kg^{-1}	Nriagu (1989)	2.0 [1.0-10] (2.3)	4-50[a]
Wildfires	Fine: 0.23 mg g^{-1} Coarse: 10.58 mg g^{-1}	This study	43 [21-210] (94)	1.2-45[a]
Industrial dust	0.01-0.05 Mn/Fe	Rathod et al. (2019)	73 [36-360] (54)	10[a]

Note. Desert and agricultural dust Mn budget values were obtained from the dust model simulations which used as input the Mn composition of soils constructed using linear interpolation from Section 2.1.1. Alternatively, soil-type extrapolation yielded 570 Gg yr-1 and 230 Gg yr-1 for desert dust and agricultural dust, respectively. [a]Nriagu (1989). [b]Mahowald et al. (2018).

2.2.1 Desert Dust

The desert dust sources of Mn refer to mineral particles entrained into the atmosphere by strong winds at the soil surface in arid unvegetated or loosely vegetated regions, where soils are prone to wind erosion, and play a major role in the global aerosol budget (Vandenbussche et al., 2020; Boucher et al., 2013; Zender et al., 2003). The emissions, transport, and deposition of dust aerosols, including seasonal and interannual variability, are all prognostic in the model. We applied the same dust emission scheme (Kok et al., 2014a, 2014b) as in Wong et al. (2021), and tuned the model to obtain a global mean aerosol optical depth (AOD) of 0.03 (Li et al., 2022) based on observational estimates (Ridley et al., 2016). Transport and deposition of Mn were simulated separately according to the size mode (Liu et al., 2016), following treatment on dust aerosols as described in Albani et al. (2014). In addition, to improve the simulation of aerosols in the coarse and accumulation modes, we modified the model by using the geometric median diameter (GMD) as that initialized in CAM5 and geomeric standard deviation as well as the edges of the predicted coarse-mode GMD following Li et al. (2022).

Because desert dust is generated from soil, we assumed that the soil Mn concentration is the same as the Mn in the dust, regardless of particle size, as we had no information on the size segregation of the soil Mn. With linear interpolation, we derived the amount of Mn emissions to be 950 Gg yr^{-1}, which was higher than 570 Gg yr^{-1} resulting from the soil map extrapolated (Table 1). Both exceeded the range (42-400 Gg yr^{-1}) provided in Nriagu (1989) and the former is comparable to the value (900 Gg yr^{-1}) given by Mahowald et al. (2018). This result indicated the high uncertainty in the amount of Mn from dust rising from different interpolation methods and the large variability in soil observations; therefore, a large range of 290-4800 Gg Mn yr^{-1} was assigned.

2.2.2 Agricultural Dust

Agricultural land use and land cover change induced by human activities can boost mineral dust emissions through various mechanisms that increase soil erodibility, such as increasingly exposing soil surface and altering hydrologic cycles (Ginoux et al., 2012; Webb & Pierre, 2018). Satellite-based analysis suggests that it represents 25% of global dust emissions (Ginoux et al., 2012). To account for agricultural dust, we applied datasets of crop fraction of present agricultural land from the Coupled Model Intercomparison Project Phase 5 (CMIP5) datasets (Hurtt et al., 2011). We separately computed the crop sources of dust (identified using the above dataset) and tuned these sources for each region to match those estimated from satellites, with the exception of Australia, where we assumed only 15% of the dust is anthropogenic, consistent with other studies (e.g., Bullard et al., 2008; Mahowald et al., 2009; Webb & Pierre, 2018). The discrepancy in Australia between the results of Ginoux et al. (2012) and other studies (Table S2) may be caused by the large drought during the time period studied by Ginoux et al. (2012). No clear evidence indicated that agriculture significantly alters the Mn concentration at the soil surface. Therefore, we assumed the same Mn fraction as desert dust and used the same approaches for estimation, deriving a global emissions of 390 Gg Mn yr^{-1} with a range of 120-1900 Gg Mn yr^{-1} (Table 1).

2.2.3 Sea spray

Sea spray aerosols are produced by the bubble-bursting process typically resulting from whitecap generation under high wind conditions in the boundary layer (O'Dowd & de Leeuw, 2007). We used prognostic sea spray included in CAM6 (Liu et al, 2011) and assumed a constant concentration of 95 μg Mn kg^{-1} in sea-spray aerosols (Nriagu, 1989). Sea-spray aerosols were estimated to emit 0.26 Gg Mn yr^{-1} with an uncertainty range of 0.13-1.3 Gg Mn yr^{-1} (Table 1), falling within the range given by Nriagu (1989).

2.2.4 Volcanoes

Studies have shown that volcanoes can be an important contributor to trace elements in aerosols, such as Mn, through eruptive activities and degassing (Mahowald et al., 2018; Sansone et al., 2002). We assumed only non-eruptive sources for this study (Spiro et al., 1992), with a constant

source across the time periods. For volcanic sources, the concentration of trace elements is commonly expressed using their ratio to sulfur (S). We adopted a mass-based ratio of 12×10^{-4} Mn/S from Nriagu (1989) and multiplied it with the concentration of sulfur given in the data set (Spiro et al., 1992) to derive Mn. We estimated non-eruptive volcanic emissions to be 3.9 Gg Mn yr^{-1} with a range of 2.0-20 Gg Mn yr^{-1}, lying at the lower end of the range provided by Nriagu (1989) (Table 1).

2.2.5 Primary Biogenic Particles

Primary biogenic particles (PBPs) are a diverse group of airborne particles such as bacteria, fungal spores, pollen, viruses and algae that are directly released from the biosphere into the atmosphere (China et al., 2020; Després et al., 2012). Like volcanoes, they are not explicitly simulated in the default CAM6 model but act as a non-negligible aerosol metal source (Mahowald et al., 2018). Following Brahney et al. (2015), we adopted parameterized PBP data that are temporally constant and based on the assumption of a leaf area index dependent source for vegetative and insect debris. We also included a pollen source based on (Heald & Spracklen, 2009) and a bacteria parameterization (Burrows et al., 2009). The emission, transport, and deposition of PBPs were simulated using a separate tracer. We assumed the Mn fraction to be 60 mg kg^{-1} in PBPs (Nriagu, 1989) and estimated its emission to be 2.0 Gg Mn yr^{-1} with a range of 1.0-10 Gg Mn yr^{-1} (Table 1).

2.2.6 Wildfires

Aerosols emitted from wildfires can significantly contribute to atmospheric Mn (Nriagu, 1989), especially in densely forested regions that are fire-prone (Krawchuk et al., 2009). Various emission datasets that use satellite-based remote sensing or other black carbon (BC) proxies are available for wildfires (van der Werf et al., 2004; Van Marle et al., 2017). Here, we employed the Coupled Model Intercomparison Project (CMIP6) wildfire dataset as the source of BC emissions (Van Marle et al., 2017), taking advantage of its coverage of both natural fires and human influence on wildfires, including deforestation fires and control of current wildfires. To convert BC to Mn concentrations, we calculated the Mn to BC ratios in coarse (PM10) and fine (PM2.5) fractions (similar to Mahowald et al., 2005; Hamilton et al., 2022) using observational data at specific sites located in the Amazon rainforest and upper southern Africa dominated by wildfires (Maenhaut et al. 1999, 2000, 2002). We derived a ratio of 10.58 mg g-1 for the coarse fraction and 0.23 mg g-1 for the fine fraction and estimated global wildfire contributions to be 43 Gg Mn yr-1 with a range of 21-210 Gg Mn yr^{-1} (Table 1). These values are higher than those reported in Nriagu (1989) based on more observations.

2.2.7 Industrial Emissions

Industrial emissions of Mn include anthropogenic fossil-fuel combustion, biomass burning, and related activities. Because Mn has many biogeochemical properties similar to those of Fe (Canfield et al., 2005), we assumed the co-occurrence of Mn with Fe and used an updated

363 detailed Fe emission inventory for 2010 developed using a Speciated Pollutant Emissions Wizard
364 (SPEW) (Bond et al., 2004; Rathod et al., 2020). This inventory covers Fe emission from fossil
365 fuel burning, wood combustion, and smelting in the industrial, transport, and residential sectors
366 globally (Alves et al., 2011; Arditsoglou et al., 2004; Block & Dams, 1976; Córdoba et al., 2012;
367 Davison et al., 1974; de Souza et al., 2010; Dreher et al., 1997; Hansen et al., 2001; Huffman et
368 al., 2000; Koukouzas et al., 2007; Linak et al., 2000a, 2000b; Machado et al., 2006; Mamane et
369 al., 1986; Martinez-Tarazona et al., 1990; Meij, 1994; Querol et al., 1995; Schmidl et al., 2008;
370 Smith et al., 1979; Steenari et al., 1999; Stegemann et al., 2000; Tsai & Tsai, 1998; Watson et al.,
371 2001; Zhang et al., 2012). We then used estimates of the ratio of Mn to Fe in each type of source
372 to obtain a new emission inventory for Mn (Table S3). Detailed data and citations are provided
373 in Data Set S3. We estimated the global industrial emission to be 73 Gg Mn yr^{-1} with a range of
374 36-360 Gg Mn yr^{-1} (Table 1). There is still a large uncertainty in these first estimates of Mn, and
375 we consider elevated sources as well in later sections to better match the observational data.
376
377 2.3 Atmospheric Observations
378 Atmospheric observations of Mn concentrations in particulate matter (PM) were compiled and
379 compared with the model output to assess the performance and tune the model. We compiled
380 atmospheric Mn observational data from a variety of global dataset networks and sites
381 (Wiedinmyer et al., 2018). The available data were collected using a variety of time periods and
382 using different chemical speciation analyses as described in detail in each study (Data Set S2).
383 Most of the data were collected with size segregation between $PM_{2.5}$ and PM_{10} size categories
384 (e.g. Hand et al., 2019). Some observational studies used coarse ($PM_{10\text{-}2.5}$ with aerodynamic
385 diameter between 2.5 and 10 μm) and fine ($PM_{2.5}$) size categories instead (e.g. Maenhaut et al.
386 1999, 2000, 2002). In this case, the two sizes were summed to compute PM_{10} for model
387 comparison. X-ray fluorescence is the most frequently used detection method to measure Mn
388 concentrations. The Mn quantification was unavailable at some stations if concentrations were
389 lower than their method detection limit (MDL). In other sites Mn was measured using
390 Inductively coupled plasma mass spectrometry (ICP-MS). In total, we obtained more data points
391 for $PM_{2.5}$ (N = 699) than PM_{10} (N = 204) because many sites focused only on $PM_{2.5}$, such as
392 from the Interagency Monitoring of Protected Visual Environments (IMPROVE) remote/rural
393 network in the US (Hand et al., 2017; Hand, 2019). Detailed descriptions of site and method, as
394 well as other elemental/total Mn PM data can be found within each referenced study (Data Set
395 S2). While there exists limited deposition elemental data, there was not enough data to warrant
396 detailed comparisons here, and the absolute values of dry deposition were often difficult to
397 measure (Prospero et al., 1996; Schutgens et al., 2016). We ignored particles larger than 10 μm
398 in aerodynamic diameter here, because of the limited data, although the missed fraction of
399 aerosols could be important for biogeochemistry in some regions (Adebiyi et al., 2023).
400
401 Hand et al. (2019) reported that collocated sites from the US Environmental Protection Agency
402 (EPA) and IMPROVE recorded different coarse aerosol mass ($PM_{10\text{-}2.5}$), with the value at EPA

sites being 10% higher than at IMPROVE sites and a 28% difference between these estimates, suggesting that different samplers could have different acuteness of size fractionation for PM_{10} and $PM_{2.5}$ (Hand et al., 2019). Overall, with a correlation coefficient of 0.9 and a slope of 0.9, the two sets of sites agreed with each other, but the difference brought by sampler biases should still be noted during later analysis and evaluation (Hand et al., 2019).

For comparison with the model, we computed annual means of atmospheric Mn concentration for each site. Particulate Mn has very low concentrations (< 1 μg-m^{-3}), and therefore in many cases the data can be below the detection limit. We applied the same procedure used by Wong et al. (2021) to correct for this potential bias. If a site had more than half of its data values above the detection limit, we set the value of any samples below MDL at this site to be one-third of the MDL (shown in dataset S2). If more than 50% of the data was below the MDL at a site, we did not include it in comparison to the model. These data were instead used to compute an upper bound based on their respective detection limits. Since many sites were close together in regions such as Europe and US, to better display the data and show the model comparison, observational data from different sites were averaged spatially within a grid cell that was two times the model resolution, or ~2° × 2° (Schutgens et al., 2016).

2.4 Estimation of "Pseudo" Turnover Time

The importance of atmospheric Mn deposition to the soil Mn reservoir was evaluated by calculating the soil Mn turnover time, which is defined as the total mass of soil Mn (estimated to 1 m depth) in each grid cell divided by the estimated atmospheric deposition flux from simulation. The Mn mass was calculated using the Mn concentration from both estimated soil maps multiplied by an average bulk density of soil, 1.4 g cm^{-3} (Yu et al., 1993). The turnover time estimated here is "pseudo-turnover time" (Wong et al., 2021) because we could not assume soil Mn to be in a steady state. The characterization of the turnover time and comparison on a global scale allowed us to assess the ecological significance of atmospheric Mn deposition in the soil Mn reservoir in units of years (Okin et al., 2004).

2.5 Correlation Analysis and Interpretation of Ecological Relevance

Whalen et al. (2018) suggested Mn limitation as a mechanism for reduced decomposition under enhanced atmospheric N deposition, therefore, it might be helpful to consider Mn deposition together with N deposition. We adopted a modeled annual N deposition dataset (2° × 2°) (Brahney et al., 2015b) and re-gridded our model output of the Mn deposition onto its resolution (2° × 2°), followed by raster calculation of the ratio of atmospheric Mn deposition to N deposition, which might provide useful insights for the relative susceptibility of soil to Mn limitation following N deposition. We compared the Mn over N ratio in deposition to the concentration ratio in soils using total N concentration data at available NCSS sites. The ratio was computed using both natural Mn deposition and total Mn deposition (natural + anthropogenic) to understand how and where human activities altered this ratio.

To examine how atmospheric Mn deposition potentially influences the Mn limitation that could be related to decomposition and soil C storage in forest ecosystems (Kranabetter et al., 2021; Moore et al., 2021; Stendahl et al., 2017; van Diepen et al., 2015; Whalen et al., 2018), we performed a spatial correlation analysis between Mn deposition and topsoil (0-5 cm) C density derived from SoilGrids 2.0, a digital soil database that includes 230,000 soil profile observations from the WoSIS and applies machine learning methods (Poggio et al., 2021) to map the global distribution of soil properties at 250 meters, resampled to our model resolution (1° × 1°). We identified the ecosystem type at each grid cell using the plant functional types in the Community Land Model, version 5 (Lawrence et al., 2019), taking the rubric of having more than 80 percent of the area covered by forest biomes. Because different forest ecosystems may have distinct soil Mn status and limitation conditions (Berg et al., 2010), they were divided into three subsystems: temperate forests, tropical forests, and boreal forests, with the correlation analysis conducted both combinedly and separately.

Because soil organic matter decomposition has long been understood to be controlled by a combination of several different factors, Mn deposition cannot be interpreted separately from other commonly outlined predictors such as precipitation (moisture), temperature, and N deposition (Berg & Matzner, 1997a; Frey et al., 2014; Hartley et al., 2021; Sierra et al., 2015; Woo & Seo, 2022; Zak et al., 2017; Zhang et al., 2019; Zhao et al., 2021b). To include these potential constraints, simple and multilinear regression analyses were carried out with the addition of the 3 other factors: precipitation, temperature (long-term mean data from Terrestrial Air Temperature and Precipitation: 1900-2014 Gridded Monthly Time Series data provided by the NOAA PSL, Boulder, Colorado, USA, from their website at *https://psl.noaa.gov*), and N deposition to test the significance of Mn deposition on topsoil C storage. The multilinear regression was calculated following the ordinary least squares (OLS) method.

3 Results

3.1 Mn Concentration in Atmospheric Particulate Matter (PM)

Mn in the model output was compared with the Mn concentration in atmospheric PM observation on a global scale. Here, we present three cases (Figures 2 and 3) for the simulation with dust emission schemes created by linear interpolation (Section 2.1.1) to better examine the model sensitivity to anthropogenic emissions. We used the bounded observational data (Section 2.3) for all comparisons and scatter plots.

The natural case (Figure 2a) was simulated without any emission from anthropogenic sources (industrial emission + agricultural dust). With only natural contributions, the model underestimated Mn concentration significantly in the PM_{10} size fraction (Figure 2b), especially over industrialized regions in Asia, Europe, and southern Africa, where the world's largest Mn mining industry is located (U.S. Geological Survey, 2022). The model also poorly simulated the

relatively high Mn concentrations reported by several sites across North America. Only close to dust desert dominated regions in North Africa does the model simulate the concentrations well (Figure 2a). The spatial distribution of Mn in western North Africa agrees with the observations on the location Mn rich dust sources (Rodríguez et al., 2020).

When anthropogenic sources were added, using the default values described in Section 2.2, the model improved the simulation in industrialized regions (Figure 3b). The value of the correlation coefficient (r) increased 3-fold with root mean squared error on the same level (RMSE) (r = 0.089, RMSE = 0.025 in Figure 2b; r = 0.27, RMSE = 0.023 in Figure 3b), suggesting that the model performance improved with the addition of anthropogenic contributions. However, Mn concentrations at the major proportion of sites were still underestimated compared with the observations. Using trial and error, we found that the atmospheric concentrations were best matched when we increased the anthropogenic emissions by a factor of 2. In comparison, adjusting natural sources only had a minimal effect on improving the overall model performance and could sometimes lower the accuracy. Natural sources other than desert dust and wildfires contributed little to the total aerosol budget (Table 1), and the most underestimated industrial regions were barely subjected to aerosol deposition associated with desert dust or wildfires. We define our “best case” as the case with elevated anthropogenic emissions (Figures 3a and b) and denoted the unmodified scenario the “low anthro” case (Figure 3c). While some stations were overestimated in the best estimate case, much fewer stations were, and the data spots were distributed more uniformly along the 1:1 line of the scatter plots, with r increased to 0.36. In many of the sites, there was a mismatch between the date of the measurement and the model simulation because of limited observations.

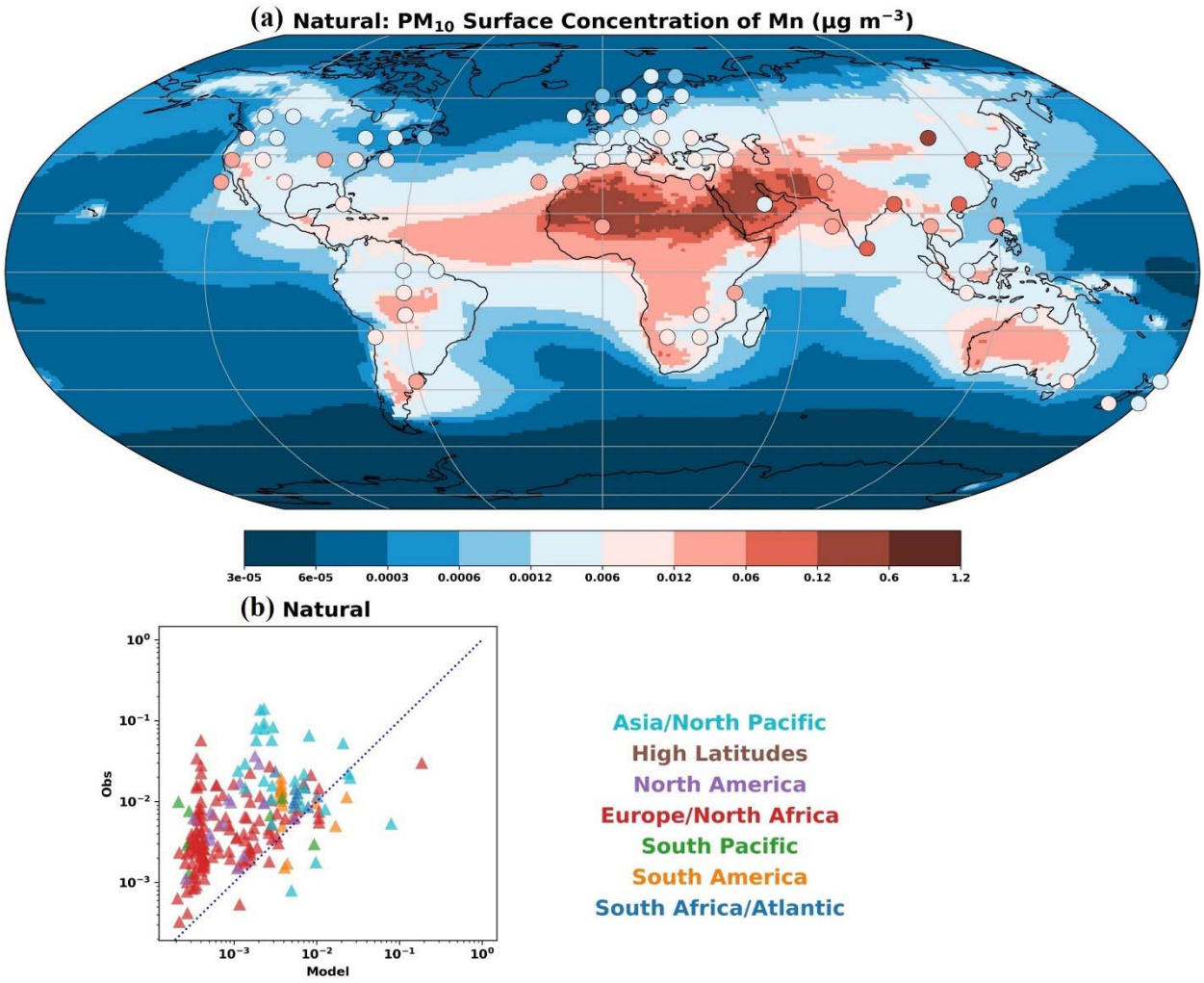

Figure 2. (a) Global distribution of the atmospheric Mn concentration at the surface in the PM_{10} size fraction from the model simulation results (contours) using only natural sources with a dust scheme constructed by linear interpolation and from bounded observations (circles). Observations were spatially averaged to a ~2° × 2° grid and compared to the Community Atmosphere Model (CAM) (v6) results. (b) Scatterplot comparison of model simulated atmospheric concentration with observations in the natural case (n = 203, r = 0.089, RMSE = 0.025). Colors of points indicate the locations of studies listed in the legend.

We noticed that a few sites with high Mn concentrations across North America including several peaks in the central United States, were still missed by the model in the best estimate case, suggesting that our estimation of anthropogenic source contributions could be lower than the actual in this region. Overall, our model agreed on the same order of magnitude of Mn concentration in atmospheric PM_{10} as the observations and had the ability to, at least, partially represent the variability in their spatial distribution.

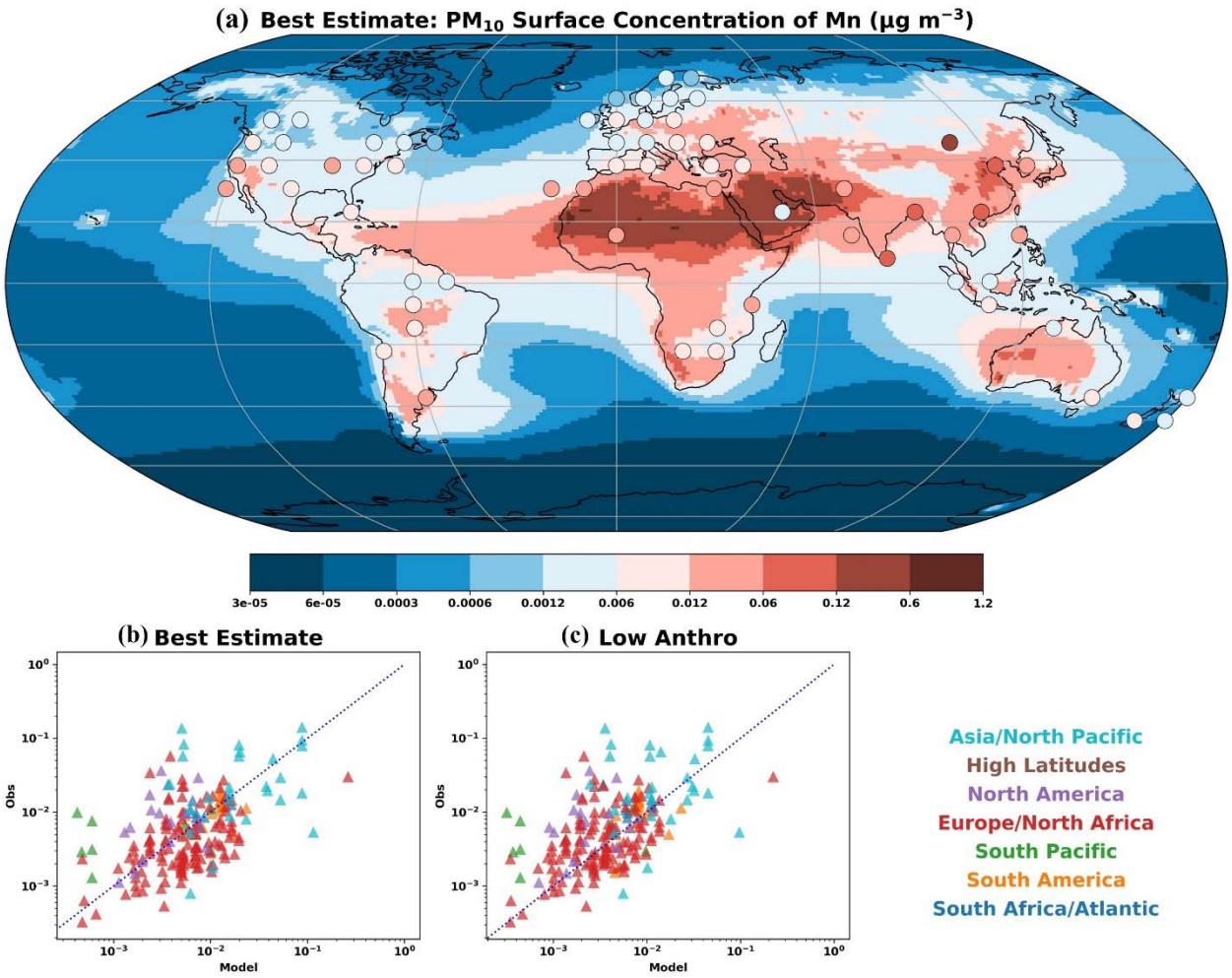

Figure 3. (a) Global distribution of the atmospheric Mn concentration at the surface in the PM_{10} size fraction from the model simulation results (contours) using the dust scheme constructed by linear interpolation in the best estimate case and from bounded observations (circles). Observations were spatially averaged to a ~2° × 2° grid and compared to the Community Atmosphere Model (CAM) (v6) results. (b) Scatterplot comparison of model simulated atmospheric concentration with observations in the best estimate case (n = 203, r = 0.36, RMSE = 0.025). Colors of points indicate the locations of studies listed in the legend. (c) Same as (b), except for the low anthropogenic model case (n = 203, r = 0.27, RMSE = 0.023).

Despite the dominance of the PM_{10} size fraction of the atmospheric Mn budget due to the coarse nature of dust (Table 1), Mn in atmospheric $PM_{2.5}$ is also important because of the high percentage of fine fraction in wildfires and industrial dust (Table 1) and the potential health risks that could be induced by inhalation of Mn in $PM_{2.5}$ in ambient air (Cavallari et al., 2008; Expósito et al., 2021). Generally, we obtained similar global distribution patterns and results of the model-observation comparison as in PM_{10}. With a more than tripled number of atmospheric Mn observations in the $PM_{2.5}$ size fraction, especially in the U.S., the model simulation better matched the observations across North America (Figure 4a). The highest observation values

were reported over industrialized regions in Europe and Asia and regions affected by desert dust generated in North Africa. Our model showed elevated atmospheric Mn levels in Europe and Asia compared to the Americas. Similarly, atmospheric Mn over industrialized regions was underrepresented by the model simulations in the natural case (Figure S2), and we derived our best estimate by tuning the level of anthropogenic emissions towards the higher end by a factor of 2. With the best estimate case, our model showed a moderately good representation of the observations (Figure 4b and c). Having more observational sites might explain the slightly better performance of the comparison in the $PM_{2.5}$ size fraction than in the PM_{10} size fraction.

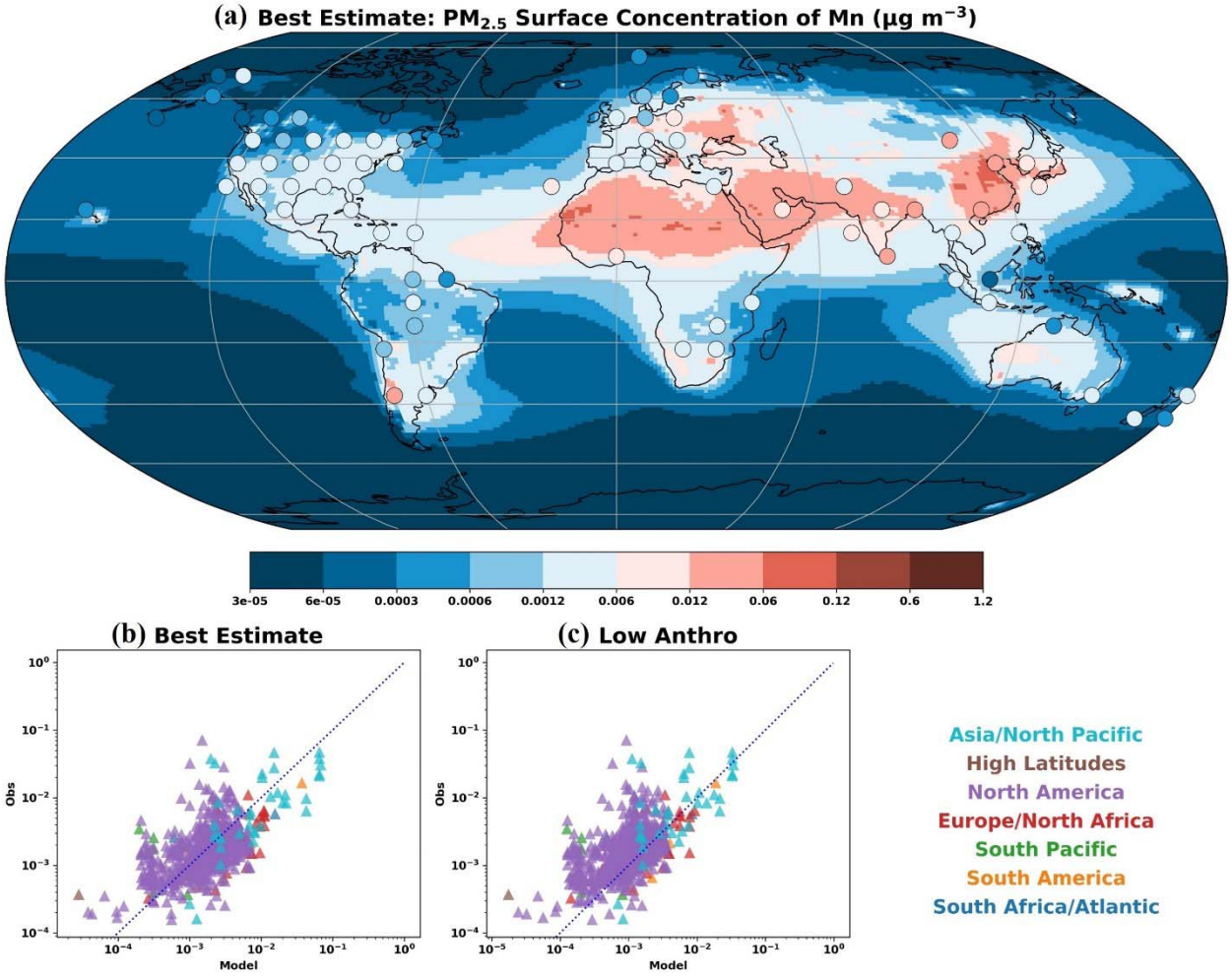

Figure 4. Same as Figure 3, but for the $PM_{2.5}$ size fraction. (a) Global distribution of the atmospheric Mn concentration at the surface from the model simulation results (contours) using the dust scheme constructed by linear interpolation in the best estimate case and from bounded observations (circles). Observations were spatially averaged to a ~2° × 2° grid and compared to the Community Atmosphere Model (CAM) (v6) results. (b) Scatterplot comparison of model simulated atmospheric concentration with observations in the best estimate case (n = 698, r = 0.53, RMSE = 0.006). Colors of points indicate the locations of studies listed in the legend. (c) Same as (b), except for the low anthropogenic model case (n = 698, r = 0.53, RMSE = 0.005).

We performed the same analysis using model simulations with a percent Mn in dust using soil-type extrapolation (Section 2.1.2) and found the results changed quantitively but not qualitatively (Figure S3). Both methods produced simulation results that were on the same order of magnitude as the observations.

3.2 Atmospheric Mn Budget and Source Apportionment

Our model predicted the global total Mn emission to be 1500 Gg Mn yr^{-1} with a range of 460-7300 Gg Mn yr^{-1} due to the uncertainty in each source (Table 1). The estimate was similar in magnitude to the reference value of 1000 Gg Mn yr^{-1} given by Mahowald et al. (2018). The model-simulated budget for each source was within or close to the estimated range from previous studies (Mahowald et al., 2018; Nriagu, 1989). The model estimated that 1000 Gg Mn yr^{-1} was emitted from natural sources with a range of 310-5000 Gg Mn yr^{-1}, while 460 Gg Mn yr^{-1} was emitted from anthropogenic sources with a range of 150-2300 Gg Mn yr^{-1} (Table 1), suggesting that approximately 32% (best estimate case) of the atmospheric Mn arose from anthropogenic contribution.

While anthropogenic sources contributed to a significant portion of the total atmospheric Mn budget, our model suggested that their main influence was in the Northern Hemisphere, where the ratio of total to natural deposition was significantly greater than 1 (Figure 5), and there was a high percentage of anthropogenic or industrial dust (Figures 6c and d), especially over industrialized regions in Asia, Europe, and the northeastern U.S. Hot spots in the Southern Hemisphere included eastern and southeastern Brazil, Peru, Chile, and southern Africa. High ratios of total to natural deposition in these regions indicated strong human perturbations (up to 10 times higher) on the Mn deposition rates (Figure 5c). Industrial emissions were responsible for major regions dominated by anthropogenic deposition, while the distribution of agricultural deposition was more dispersed, with a wider coverage of cultivated areas worldwide (Figures 6c and d).

Desert dust represented over 90% of all natural sources of the atmospheric Mn deposition (Table 1). It dominated deposition within major deserts in North Africa, inland Australia, and Asia as well as regions that were affected by the transportation of desert dust produced in these systems (Kellogg & Griffin, 2006). For example, the intercontinental transport of African dust to South America has been identified as an important source of new atmospheric deposition of P in the Amazon and could have a fertilization effect (Okin et al., 2004; Ridley et al., 2012; Yu et al., 2015). The dominance of desert dust and other natural sources (sea salts and volcanoes, which represented a very small fraction) was complementary with anthropogenic sources: desert dust dominated most of the Southern Hemisphere but became less influential at higher latitudes in the Northern Hemisphere as anthropogenic emissions concentrated there (Figure 6a).

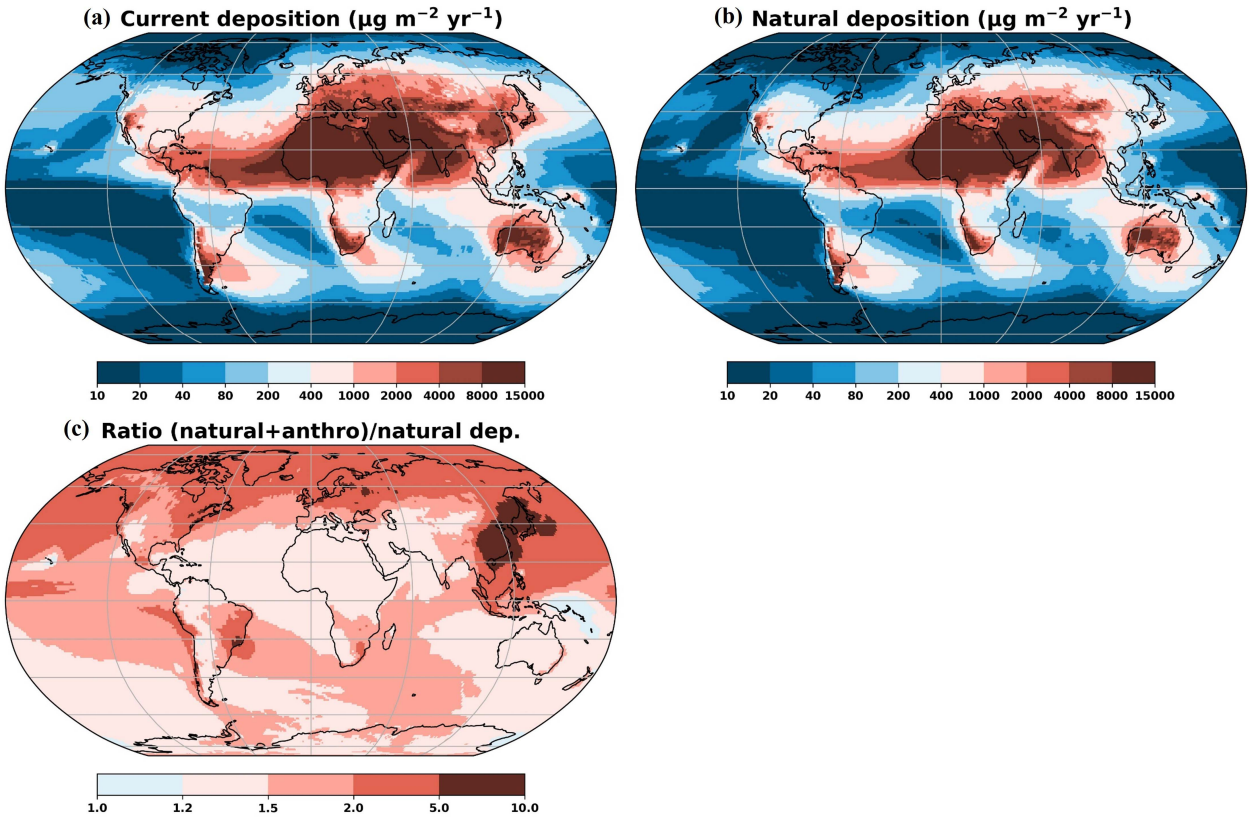

Figure 5. (a) Global pattern of the current (anthropogenic + natural sources) atmospheric Mn deposition (μg m^{-2} yr^{-1}) as simulated in the Community Atmosphere Model (CAM) (v6) in the best estimate case. (b) Same as (a), except for including natural sources of emissions only. (c) Ratio of total atmospheric Mn deposition to natural deposition.

Although wildfires have a much lower budget than desert dust, they are the second-largest natural source of atmospheric Mn (Table 1). Together with primary biogenic particles, they dominated regions such as the Amazon rainforest, upper southern Africa (and Madagascar), Indonesia, northern Canada and Alaska (Figure 6b). Wildfires can displace large amounts of nutrients, including Mn, from terrestrial ecosystems (Kauffman et al., 1995; Mahowald et al., 2005) which were then replenished by transported dust and sea salts, as well as anthropogenic depositions, similar to what was reported by Wong et al. (2021) in the case of molybdenum (Mo).

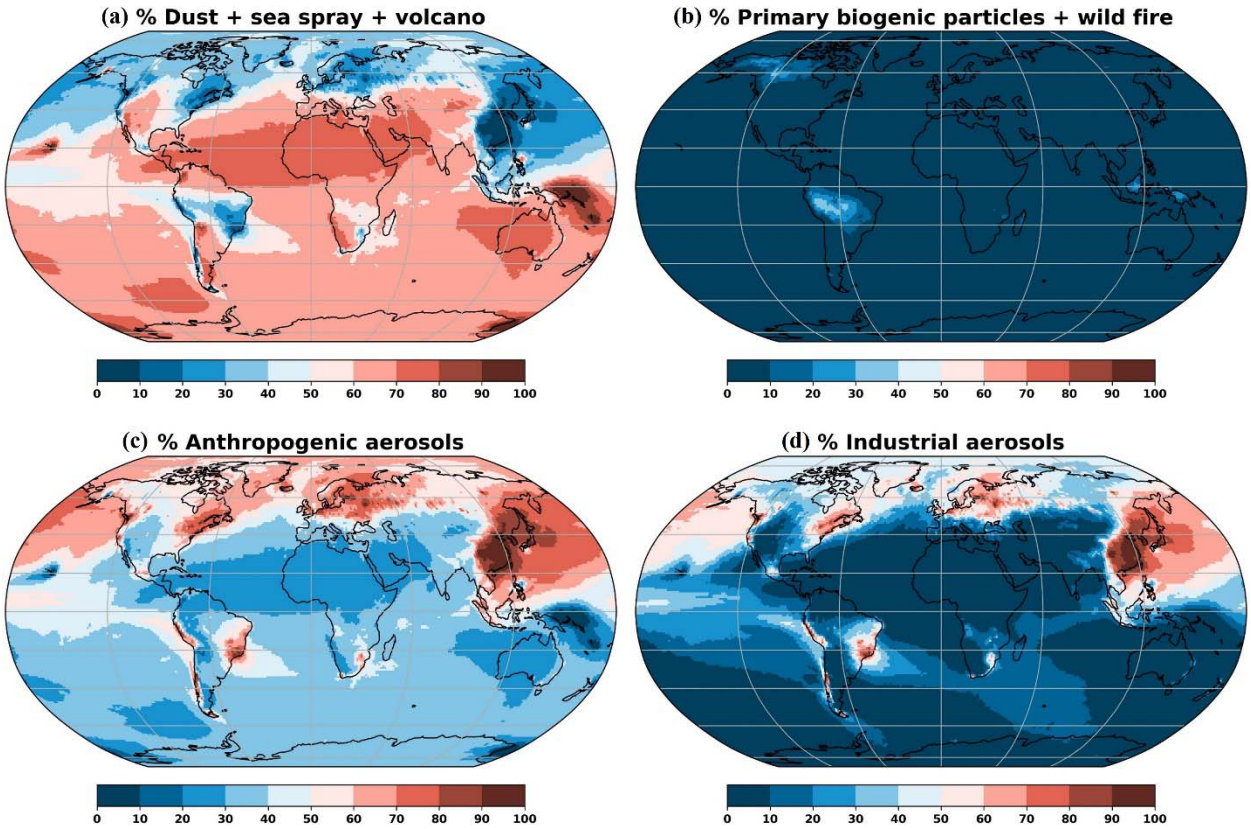

Figure 6. Source apportionment of the atmospheric Mn deposition in the best estimate case shown by percentage of different sources in the Community Atmosphere Model (CAM) (v6): (a) desert dust, sea sprays, and volcanoes, (b) primary biogenic particles and wildfires, (c) combined anthropogenic aerosols (agricultural dust + industrial emissions) and (d) industrial aerosols.

3.3 Soil Mn "Pseudo Turnover" Times

The "pseudo" turnover time provides a metric of the ecological importance of atmospheric Mn deposition to the topsoil Mn reservoir (Okin et al., 2004). Using the two approaches (Section 2.1), we divided the estimated soil Mn concentration by the model simulated Mn deposition rates to compute "pseudo" turnover times in topsoils (Okin et al., 2004). The estimated soil Mn "pseudo" turnover time varied spatially, ranging from 1,000-10,000 years in regions dominated by desert dust to over 10,000,000 years at higher latitudes (Figures 7a and b). We found that anthropogenic sources significantly shortened the soil Mn "pseudo" turnover times in industrialized regions regardless of the interpolation method. For example, the atmospheric deposition sourced from anthropogenic emissions shortened the soil Mn "pseudo" turnover time by 1-2 orders of magnitude from millions of years to as low as tens of thousands of years in eastern China and across Europe (Figures 7a and c; b and d). These trends indicate that human perturbation has the potential to accelerate Mn turnover in different terrestrial systems if the amount of anthropogenic activity remains at the same level or even rises in the future.

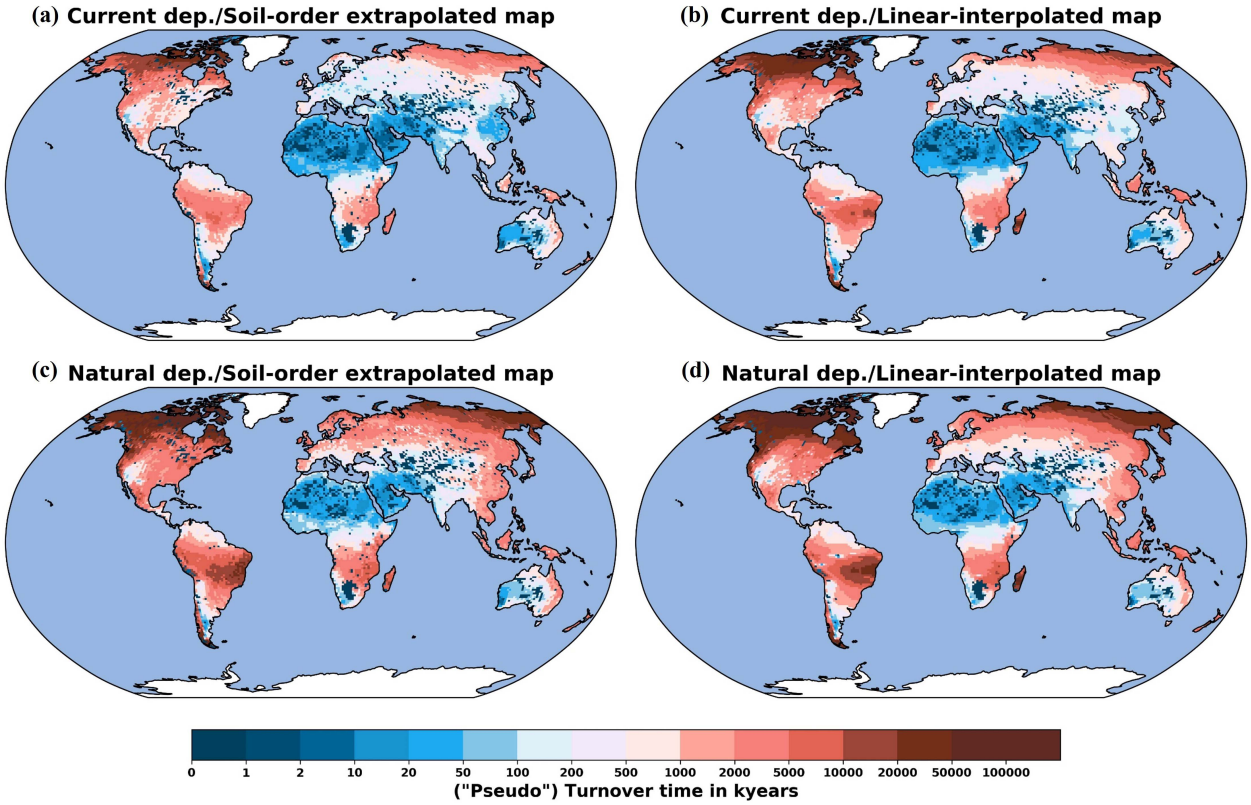

Figure 7. "Pseudo" turnover times (kiloyears) of the surface soil Mn from current (natural + anthropogenic sources) atmospheric Mn deposition as simulated in the Community Atmosphere Model (CAM) (v6) using the dust scheme constructed from (a) linear interpolation (and calculated using the linear-interpolated soil Mn map) and (b) soil order extrapolation (and calculated using the soil-order extrapolated soil Mn map). (c and d) Same as (a and b) except for the inclusion of only natural Mn deposition in the calculation of turnover times.

Compared to the Mo "pseudo" turnover time of 1,000-2000,000 years (Wong et al., 2021), the estimated range of soil Mn "pseudo" turnover times was wider, and the mean turnover time was longer, which is closer to the estimated range of P "pseudo" turnover time (~10^4 to ~10^7 years) in Okin et al. (2004). In the Amazon region, the soil Mn "pseudo" turnover time ranged from hundreds of kiloyears in the northeast corner, which was subject to deposition from transported African dust, to thousands of kiloyears moving toward the central and southwestern regions. Compared to the turnover times from other studies of macronutrients, the estimated Mn "pseudo" turnover time here was orders of magnitude longer than the N turnover time of 177 years globally (Rosswall, 1976) and the P turnover time of 50 years averaged across several stations in the Amazon rain forest (Mahowald et al., 2005), which was accelerated by human-induced land use change such as deforestation and biomass burning (Andela et al., 2017; Hansen et al., 2013). Overall, these comparisons illustrate the spatial variability of the soil Mn "pseudo" turnover times and suggest that atmospheric deposition of Mn may play a non-negligible role in the terrestrial surface Mn cycle in many regions world-wide.

653
654 3.4 Linkage to N deposition and C storage
655 3.4.1 Mn to N Ratio in Deposition
656 In addition to characterizing the atmospheric Mn cycle itself, it is important to look at its linkage
657 to the biogeochemical cycles of two major elements, C and N. The Mn limitation has been
658 proposed to explain the reduced organic matter decomposition in soils under chronic atmospheric
659 N deposition (Moore et al., 2021; Whalen et al., 2018), which has the potential to regulate carbon
660 sequestration in forest soils. Therefore, using the N deposition/concentration ratio to normalize
661 the Mn deposition/concentration ratio (deriving Mn-to-N ratios) could make our results more
662 interpretive in such a way that it could reveal the soil's vulnerability to the Mn limitation (if N is
663 sufficient) and thus relates to soil C dynamics. As anthropogenic emissions have significantly
664 perturbed the cycling of atmospheric N (Dentener et al., 2006; Galloway et al., 2014; Kanakidou
665 et al., 2016) and Mn, it is likely that humans have also altered this ratio of Mn to N, affecting soil
666 C accumulations and introducing further feedbacks on climate.
667
668 The ratio of Mn to N in the atmospheric deposition varies globally by several orders of
669 magnitude. It could be as low as 5×10^{-5} in the northern latitudes and over 0.02 in desert dust
670 dominated regions, where there is little nitrogen fixation in soils, and the dust composition is
671 almost entirely of mineral nature (Davies-Barnard & Friedlingstein, 2020). Anthropogenic
672 emissions increased the depositional ratio of Mn to N in most parts of the world (even in
673 Antarctica), with the impact in industrialized regions being the most substantial (Figure 8a).
674 When only considering the natural sources, we estimated that the Mn-to-N ratio is moderately
675 low in major industrialized regions including northern Europe, eastern China, and the
676 northeastern U.S., with the U.S. having lower ratios than Asia and Europe in general (Figure 8b).
677 Anthropogenic sources enhanced the Mn-to-N ratio in all these regions, with a stronger effect in
678 China and Europe than in the U.S. Other areas with low Mn-to-N ratio under current deposition
679 were either around the equator, where much nitrogen fixation occurred (Davies-Barnard &
680 Friedlingstein, 2020), or at higher latitudes. These regions were generally affected only by desert
681 and anthropogenic dust and had relatively large wildfire and PBP contributions in deposition
682 (Figure 6b). This could be best illustrated in the Amazon forest, where the northernmost portion
683 influenced by African dust transportation (Ridley et al., 2012) had a much higher Mn-to-N ratio
684 than the central part (Figures 8a and b).

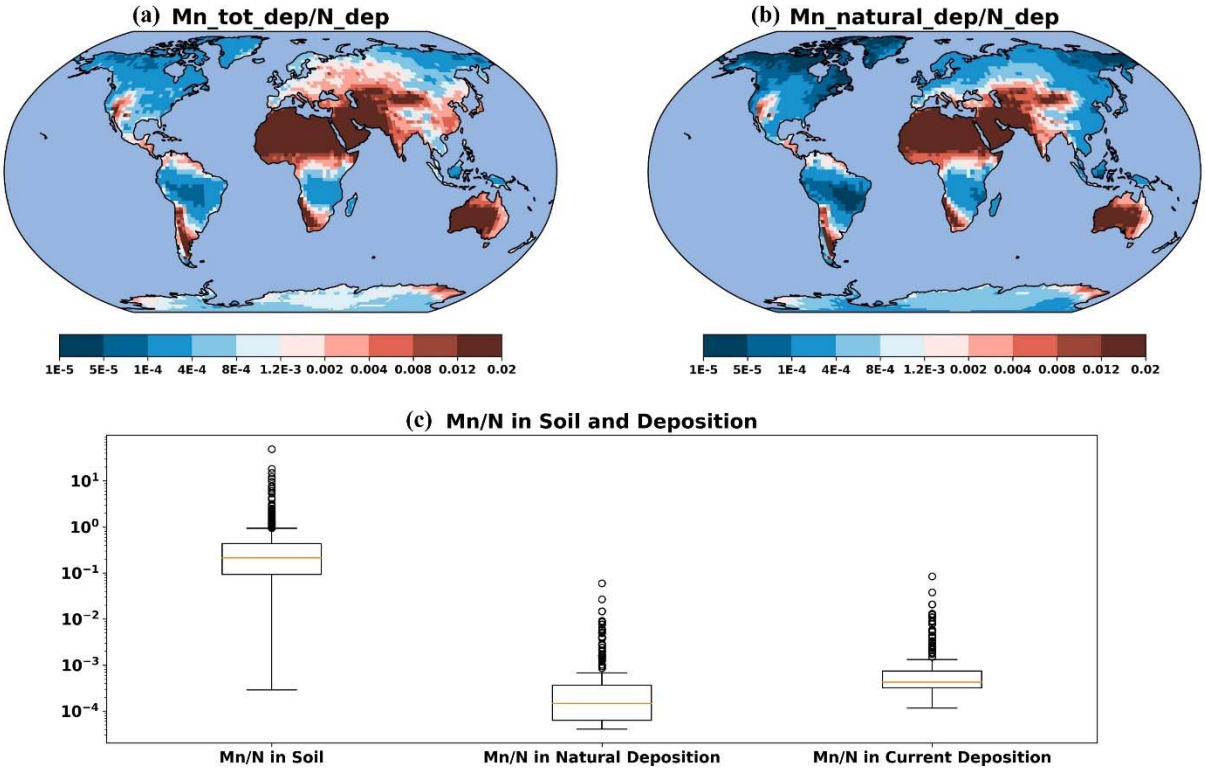

Figure 8. (a) Ratio of Mn to N in atmospheric deposition calculated using the current Mn deposition simulated in the Community Atmosphere Model (CAM) (v6) and the N deposition from Brahney et al. (2015b). (b) Same as in (a), except for the inclusion of only natural Mn deposition in the calculation. (c) Box plot showing the Mn-to-N ratio in surficial soils at available sites and in depositions (current + natural).

We compared the M-to-N ratio in atmospheric deposition to the in-situ ratio of Mn to N concentration in surficial soils at 1319 available sites (mainly across the U.S.). For example, Kranabetter et al. (2021) reported 541 mg kg^{-1} Mn and 0.77% total N in surficial soils in a temperate forest located on southern Vancouver Island. With the measurements in the abovementioned study, we calculated the in-situ Mn-to-N ratio in soil to be 0.068, which was over two orders of magnitude larger than the depositional Mn-to-N ratio of 0.00052 calculated using our gridded model output and the N deposition dataset (extracting the value of the grid in which Vancouver Island was located). Considering all available soil observational sites that contained valid measurements of Mn and N concentrations (mainly from the NCSS dataset), we obtained a median depositional Mn-to-N ratio of 0.00042 versus a median soil Mn-to-N ratio of 0.21. We found that the current depositional ratio was typically one to three orders of magnitude lower than the soil concentration ratio, and the difference was larger with natural deposition (Figure 8c). Considering the relatively higher Mn-to-N ratio in soils, regions with disproportionally low Mn-to-N ratios in atmospheric deposition were interpreted to be the most vulnerable to potential Mn limitation (if deposition makes soil N sufficient), such as temperate

and boreal forests in northeastern U.S., Canada, and northern Europe, in agreement with current field experimental results (Kranabetter et al., 2021; Stendahl et al., 2017; Whalen et al., 2018).

3.4.2 Correlation with Topsoil C Density

To test the significance of atmospheric Mn deposition in removing soil Mn limitation and thus facilitating decomposition in forest ecosystems on a global scale, we correlated our simulated atmospheric Mn deposition with the topsoil (0-5 cm) C density derived from SoilGrids 2.0 (Poggio et al., 2021), with both values extracted from grid cells where the plant functional type was identified as (sub)tropical, temperate, or boreal forest. In each case, a simple linear regression between topsoil C density and each of the four factors was carried out, including Mn deposition. Our results revealed fairly good negative correlations ($r < -0.5$) between C density and Mn deposition in temperate ($r = -0.67$) and (sub)tropical forests ($r = -0.54$; Figure 9a). A similar negative relationship was determined between C density and N deposition in temperate forests ($r = -0.69$; Figure 10b), where a significant positive relationship was obtained in the case of precipitation ($r = 0.71$; Figure 10d). In addition, a negative correlation between C density and temperature was found only in subtropical forest, though relatively weaker ($r = -0.46$; Figure 10c). When we combined the three forest ecosystems for simple regression analysis, all factors showed statistically significant correlation, with Mn deposition ($r = -0.37$, $p < 0.0001$) having the third strongest coefficient of determination (Table 2).

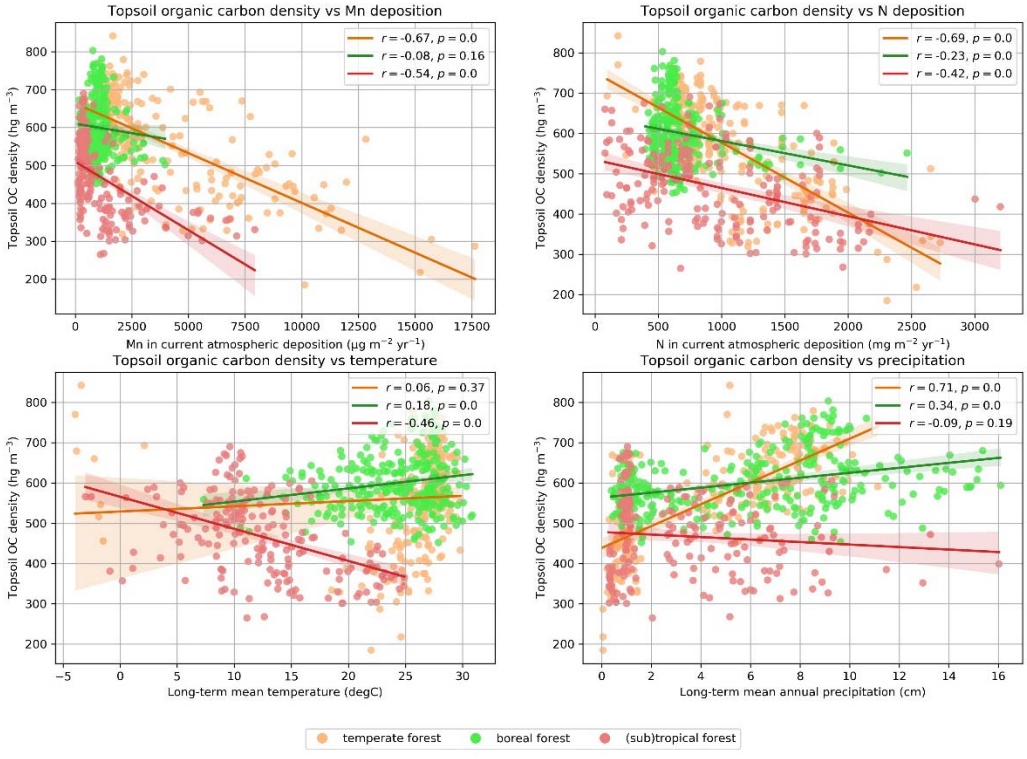

Figure 9. Scatterplots with simple linear regression lines between topsoil (0-5 cm) C density (hg m^{-3}) and (a) Mn in current atmospheric deposition (μg m^{-2} yr^{-1}), (b) N in current atmospheric deposition (mg m^{-2} yr^{-1}), (c) long-term mean temperature (°C), and (d) long-term mean annual

precipitation (cm) in temperate, boreal, and tropical forests. "*P = 0.0*" legend suggests a p-value < 0.0001.

Results from multilinear regression confirmed the negative relationship between C density and Mn deposition to remain statistically significant along with the inclusion of the other factors into the model (Table 2). Overall, the R-squared value of the OLS model reached 0.434, with the skew (-0.115), kurtosis (3.033), and Jarque-Bera test (1.506, p = 0.471) likely indicating normally distributed residuals. To check for multicollinearity, we computed a correlation matrix (Table S4) and found a positive correlation between Mn deposition and N deposition (r = 0.61, p < 0.0001), providing the possibility that the negative correlation between C storage and Mn deposition was a "byproduct" of the positive correlation between Mn and N deposition. A calculation of variance inflation factors (VIF) obtained values < 2 for all individual variables (Table S4), suggesting that variables were only moderately correlated with each other, and multicollinearity was likely not problematic. Therefore, it is reasonable to conclude that the Mn deposition could be a predictor of topsoil C density along with N deposition and other climatic factors in forest ecosystems (predominantly temperate and tropical). In fact, Mn addition to soils has been shown to increase C losses (e.g., CO_2 and dissolved organic carbon) during litter decomposition, suggesting increased Mn supply could result in decreased soil C storage (Trum et al., 2015; Jones et al., 2020).

Table 2

Result statistics of simple and multilinear regression between topsoil C content and Mn deposition, N deposition, temperature, and precipitation.

Variable Name	**Simple linear regression**		**multilinear regression**		
	r	**p-value**	**coef**	**t**	**P > |t|**
Intercept			500.2603	39.248	0.000
Mn deposition	-0.372	< 0.0001	-0.0085	-4.369	0.000
N deposition	-0.493	< 0.0001	-0.0693	-7.977	0.000
Temperature	0.270	< 0.0001	4.1265	9.313	0.000
Precipitation	0.472	< 0.0001	8.8977	9.964	0.000

4 Discussion

4.1 Model-observation Discrepancy

Although our model simulation results had a moderately good representation of the atmospheric observations under the best estimate scenario, many stations were still under- or over-predicted (Figures 4 and 5). The discrepancy between the model and observations could arise from a variety of processes, with errors in the sources, deposition or transport pathways all contributing (Mahowald et al., 2011; Loosmore, 2003). For example, we were not able to include the emissions from direct volcanic eruptions due to the lack of data and thus constrained to apply non-eruptive degassing data only. Errors in estimates of dust deposition are thought to be of order of a factor of 10 (Mahowald et al., 2011). Because we derived Mn from industrial sources

765 from a correlation with Fe (since these are the only spatially explicit mining emissions available:
766 Rathod et al., 2019), emissions from nonferrous industries such as silico-manganese alloy,
767 synthetic pyrolusite, and Mn chemical manufacturing plants were neglected (Parekh, 1990).
768 Estimates of fugitive emissions from mining are not available, and thus not included in this study.
769
770 Another limitation was that, except for desert and agricultural dust, we used a constant emission
771 factor for each source because we did not have sufficient data to assess the spatial variability of
772 the Mn emission factors from different sources such as PBP, sea sprays, and volcanoes, which
773 could vary within the ranges given in Nriagu (1989). For example, trace element composition
774 can vary in materials formed by biological production in different water masses (Kuss &
775 Kremling, 1999). With the constant emission factor assumption, our model could over- or
776 underestimate the observations, depending on the location of the site and its source
777 apportionment.
778
779 Our regression model was not able to determine a statistically significant negative correlation
780 between topsoil C density and our simulated atmospheric Mn deposition in boreal forests. This
781 seems contradictory with the results from a direct observational study carried out in northern
782 Swedish boreal forests, where Mn was found to act as a critical factor regulating C accumulation
783 (Stendahl et al., 2017). This apparent discrepancy might be attributed to the limited number of
784 soil observations within the boreal regime, introducing large uncertainty at the higher latitudes in
785 our linear-interpolated soil map, thus reducing the model's ability to accurately predict the
786 relationship in boreal ecosystems on a global scale. With most soil observations located around
787 the middle latitudes, it would not be surprising that our model has the greatest confidence there.
788
789 4.2 Anthropogenic Perturbation and Implications for C Cycling
790 Our model and observations suggest that anthropogenic perturbations played an important role in
791 global atmospheric Mn cycling, for which 32% of the total emissions were attributed to
792 anthropogenic sources. As the dominant contributor of emissions in most industrialized regions,
793 the influence of anthropogenic sources could be equal to or exceed that of natural sources,
794 especially in the northern hemisphere (Figure 7), where they significantly accelerated the Mn
795 turnover times in surficial soils by enriching the atmospheric deposition in which the Mn-to-N
796 ratio was boosted. Human activities, including industrialization and agricultural practices, likely
797 alter Mn cycles by a factor of two or more in many associated areas (Figure 6), on the same order
798 of magnitude as the perturbation to the cycling of other metals such as Mo, aluminum (Al), lead
799 (Pb), mercury (Hg), and vanadium (V) (Rauch & Pacyna, 2009; Schlesinger et al., 2017; Selin,
800 2009; Sen & Peucker-Ehrenbrink, 2012; Wong et al., 2021).
801
802 Our results reinforce the negative correlation between Mn and soil C storage in temperate and
803 boreal forests on a global scale (Kranabetter et al., 2021; Stendahl et al., 2017), indicating that
804 the Mn availability is likely a limiting factor on the soil organic matter decomposition that

consumed C from storage in these ecosystems. This implies that if atmospheric deposition is the major source of Mn in surficial soil layers, it has the potential to facilitate oxidative C decomposition by removing the limitation by Mn, and in regions that are sensitive to anthropogenic activities, humans might indirectly alter the C cycle by releasing aerosols composed of Mn into the atmosphere through industrial and agricultural activities. While a significant proportion of global C is stocked in the soils and vegetation of boreal and temperate forests in combination (IPCC, 2000), increased C emissions in these systems from decomposition promoted by Mn addition could be important to global C dynamics and climate feedbacks, exacerbating the ongoing escalating C emissions in boreal forests subjected to wildfires (Phillips et al., 2022; Zhao et al., 2021a).

However, to quantitatively characterize the extent of the Mn deposition's influence on C cycling, more field measurements and experimental studies are required. For example, our current understanding would be improved if soil organic matters at different stages of decomposition could be distinguished. Berg et al. (2007) points out that Mn addition has a stronger effect on late-stage decomposition by enhancing lignin-degrading enzymes because microbes tend to decompose lignin after the more labile organic substrates (Berg, 2014; Berg & Matzner, 1997). In addition, we focused on modelling the total extractable and/or acid digested Mn in soils and atmospheric deposition and did not consider Mn bioavailability explicitly, which is crucial to the microorganisms that are responsible for decomposition and can be regulated by the cycling of Mn in different oxidation states (Keiluweit et al., 2015). Incorporation of mechanisms constraining the bioavailability, mobility, and reactivity of Mn (Keiluweit et al., 2015) in future model calibrations is essential for a more accurate interpretation. Finally, our estimated "pseudo" turnover time and the Mn-to-N ratio could only partially represent the Mn status in soils because we did not include fluxes from other reservoirs in the Mn cycle. For instance, release of Mn(II) from clay mineral weathering and Mn(III, IV)-oxide reduction (Canfield et al., 2005) could increase the available Mn concentration in soils, creating the gap between the Mn-to-N ratio in deposition and in soils.

4.3 Limitations of the Observational Data

Our collected atmospheric observations of Mn are spread over 6 out of 7 continents, but high spatial coverage is mostly restricted to industrialized countries. To improve our understanding of atmospheric contribution to the Mn cycle, more observations of the concentration and deposition in currently less-observed areas such as the polar regions are needed to further constrain the tuning of the model.

There are more locations with soil Mn measurements than atmospheric observations, but they are concentrated mostly in Europe and the U.S. Because of the uneven distribution of the soil observations and the limited number of them across many countries, we are not able to capture the variability of the soil Mn concentration at small scale. For example, we did not include

measurements of Mn concentration at metal-contaminated sites associated with mining or other industries (Lv et al., 2022) in either interpolation approach. With the currently available soil data, the linear interpolation approach is uncertain in areas where in-situ soil observations are sparse and less representative, whereas the problem with soil order extrapolation is that several soil orders show a lack of sufficient measurements to calibrate the median value. While we gained a better estimation of the dust emission scheme with a soil order extrapolation in our specific case, many studies (Baize, 2010; Wong et al., 2018; Okin et al., 2008) have shown that suggested that soil orders, which are the highest level of taxonomic classification, are typically inadequate when dealing with trace element concentrations in soils, and the intra-order variation could be large. Better estimation might be achieved with more refined classification at lower taxonomic levels such as suborders and great groups, or even quantitatively with particle size distribution. However, fewer sites specify the abovementioned information, and at such levels, the conversion between different classification systems is more complex.

5 Conclusions

In this study, we present, for the first time, a spatially explicit estimation of the global atmospheric Mn sources, distribution, and deposition using a combined model-observation approach. We estimate that anthropogenic sources (390 Gg Mn yr^{-1}) represent approximately 32% of the total atmospheric Mn budget (1500 Gg Mn yr^{-1}). Including this portion of Mn emissions in the model enhanced Mn deposition in many industrialized regions, which could accelerate soil Mn turnover as high as 100-fold and boost the Mn-to-N ratio in atmospheric deposition. Deposition of the anthropogenic Mn from human activities have a high potential to facilitate SOM decomposition in temperate and (sub)tropical forest ecosystems, thus influencing C storage and the global C cycle. Given the sparsity of observations and limited understanding of atmospheric Mn sources, uncertainties are high in these estimations. We need more atmospheric and soil observations across different landscapes to refine our model in the future and thus quantification of the global Mn cycle.

Acknowledgments

NMM and LL would like to acknowledge the support of DOE grant: DE-SC0021302. SR acknowledges the support of grants AEROEXTREME PID2021-125669NB-I00, AEROATLAN CGL 2015-66299-P & POLLINDUST CGL2011-26259 funded by ERDF and the Research State Agency of Spain.

Data Availability Statement

Observational synthesis available in the supplemental materials, while model results are available at the Cornell eCommons repository.

References

Abanda, P. A., Compton, J. S., & Hannigan, R. E. (2011). Soil nutrient content, above-ground biomass and litter in a semi-arid shrubland, South Africa. *Geoderma*, *164*(3–4), 128–137. https://doi.org/10.1016/j.geoderma.2011.05.015

Adebiyi, A., Kok, J. F., Murray, B. J., Ryder, C. L., Stuut, J.-B. W., Kahn, R. A., Knippertz, P., Formenti, P., Mahowald, N. M., Pérez García-Pando, C., Klose, M., Ansmann, A., Samset, B. H., Ito, A., Balkanski, Y., Di Biagio, C., Romanias, M. N., Huang, Y., & Meng, J. (2023). A review of coarse mineral dust in the Earth system. *Aeolian Research*, *60*, 100849. https://doi.org/10.1016/j.aeolia.2022.100849

Albani, S., Mahowald, N. M., Perry, A. T., Scanza, R. A., Zender, C. S., Heavens, N. G., Maggi, V., Kok, J. F., & Otto-Bliesner, B. L. (2014). *Journal of Advances in Modelling Earth Systems*, *6*(3), 541-570. https://doi.org/10.1002/2013MS000279

Alfaro, M. R., Montero, A., Ugarte, M. O., do Nascimento, C. W. A., de Aguiar Accioly, A. M., Biondi, C. M., & da Silva, Y. J. (2015). Background concentrations and reference values for heavy metals in soils of Cuba. *Environmental Monitoring and Assessment*, *187*(1). https://doi.org/10.1007/s10661-014-4198-3

Alongi, D. M., Wattayakorn, G., Boyle, S., Tirendi, F., & Payn C and Dixon, P. (2004). Influence of roots and climate on mineral and trace element storage and flux in tropical mangrove soils. *Biogeochemistry 69*(1), 105–123. https://doi.org/10.1023/B:BIOG.0000031043.06245.af

Alves, C., Gonçalves, C., Fernandes, A. P., Tarelho, L., & Pio, C. (2011). Fireplace and woodstove fine particle emissions from combustion of western Mediterranean wood types. *Atmospheric Research*, *101*(3), 692–700. https://doi.org/10.1016/j.atmosres.2011.04.015

905 Andela, N., Morton, D. C., Giglio, L., Chen, Y., van der Werf, G. R., Kasibhatla, P. S., DeFries,
906 R. S., Collatz, G. J., Hantson, S., Kloster, S., Bachelet, D., Forrest, M., Lasslop, G., Li, F.,
907 Mangeon, S., Melton, J. R., Yue, C., & Randerson, J. T. (2017). A human-driven decline in
908 global burned area. *Science*, *356*(6345), 1356–1362. https://doi.org/10.1126/science.aal4108
909 Andruszczak, E. (1975). Zawartość makro- i mikroelementów w glebach i roślinności użytków
910 rolnych Kotliny Kłodzkiej. *Roczniki Gleboznawcze*, *26*(3).
911 Arditsoglou, A., Petaloti, C., Terzi, E., Sofoniou, M., & Samara, C. (2004). Size distribution of
912 trace elements and polycyclic aromatic hydrocarbons in fly ashes generated in Greek lignite-fired
913 power plants. *The Science of the Total Environment*, *323*, 153–167.
914 https://doi.org/10.1016/j.scitotenv.2003.10.013
915 Asawalam, D. O., & Johnson, S. (2007). Physical and chemical characteristics of soils modified
916 by earthworms and termites. *Communications in Soil Science and Plant Analysis*, *38*(3–4), 513–
917 521. https://doi.org/10.1080/00103620601174569
918 Baize, D. (2010). *Concentrations of trace elements in soils: The three keys*. IUSS-International
919 Union of Soil Sciences. https://www.researchgate.net/publication/275645543
920 Batjes, N. H. (1997). A world data set of derived soil properties by FAO-UNESCO soil unit for
921 global modelling. *Soil Use and Management*, *13*, pp. 9-16.
922 Becquer, T., Quantin, C., & Boudot, J. P. (2010). Toxic levels of metals in Ferralsols under
923 natural vegetation and crops in New Caledonia. *European Journal of Soil Science*, *61*(6), 994–
924 1004. https://doi.org/10.1111/j.1365-2389.2010.01294.x
925 Berg, B. (2014). Decomposition patterns for foliar litter – A theory for influencing factors. *Soil*
926 *Biology and Biochemistry*, *78*, 222–232. https://doi.org/10.1016/j.soilbio.2014.08.005

927 Berg, B., Davey, M. P., de Marco, A., Emmett, B., Faituri, M., Hobbie, S. E., Johansson, M. B.,
928 Liu, C., McClaugherty, C., Norell, L., Rutigliano, F. A., Vesterdal, L., & Virzo De Santo, A.
929 (2010). Factors influencing limit values for pine needle litter decomposition: A synthesis for
930 boreal and temperate pine forest systems. *Biogeochemistry*, *100*(1), 57–73.
931 https://doi.org/10.1007/s10533-009-9404-y
932 Berg, B. (2000). Litter decomposition and organic matter turnover in northern forest soils. *Forest*
933 *Ecology and Management*, 133(1-2), 13-22. https://doi.org/10.1016/S0378-1127(99)00294-7
934 Berg, B., & Matzner, E. (1997). Effect of N deposition on decomposition of plant litter and soil
935 organic matter in forest systems. *Environmental Reviews*, *5*(1), 1–25.
936 https://doi.org/10.1139/a96-017
937 Berg, B., Steffen, K. T., & McClaugherty, C. (2007). Litter decomposition rate is dependent on
938 litter Mn concentrations. *Biogeochemistry*, *82*(1), 29–39. https://doi.org/10.1007/s10533-006-
939 9050-6
940 Beygi, M., & Jalali, M. (2018). Background levels of some trace elements in calcareous soils of
941 the Hamedan Province, Iran. *Catena*, *162*, 303–316.
942 https://doi.org/https://doi.org/10.1016/j.catena.2017.11.001
943 Bibak, A., Moberg, J. P., & Borggaard, O. K. (1994). Content and distribution of cobalt, copper,
944 manganese and molybdenum in Danish spodosols and ultisols. *Acta Agriculturae Scandinavica,*
945 *Section B — Soil & Plant Science*, *44*(4), 208–213. https://doi.org/10.1080/09064719409410247
946 Block, C., & Dams, R. (1976). Study of fly ash emission during combustion of coal.
947 *Environmental Science & Technology*, *10*(10), 1011–1017. https://doi.org/10.1021/es60121a013

948 Boente, C., Matanzas, N., García-González, N., Rodríguez-Valdés, E., & Gallego, J. R. (2017).
949 Trace elements of concern affecting urban agriculture in industrialized areas: A multivariate
950 approach. *Chemosphere*, *183*, 546–556. https://doi.org/10.1016/j.chemosphere.2017.05.129
951 Bond, T. C., Streets, D. G., Yarber, K. F., Nelson, S. M., Woo, J. H., & Klimont, Z. (2004). A
952 technology-based global inventory of black and organic carbon emissions from combustion.
953 *Journal of Geophysical Research: Atmospheres*, *109*(14). https://doi.org/10.1029/2003JD003697
954 Boucher, O., D. Randall, P. Artaxo, C. Bretherton, G. Feingold, P. Forster, V.-M. Kerminen, Y.
955 Kondo, H. Liao, U. Lohmann, P. Rasch, S.K. Satheesh, S. Sherwood, B. Stevens, & Zhang X. Y.
956 (2013). Clouds and aerosols. In T.F. Stocker, D. Qin, G.-K. Plattner, M. Tignor, S.K. Allen, J.
957 Doschung, A. Nauels, Y. Xia, V. Bex, and P.M. Midgley (Eds.), *Climate Change 2013: The*
958 *Physical Science Basis. Contribution of Working Group I to the Fifth Assessment Report of the*
959 *Intergovernmental Panel on Climate Change* (pp. 571-657). Cambridge University Press.
960 https://doi.org/10.1017/CBO9781107415324.016.
961 Bradford, G. R., Chang, A. C., Page, A. L., Bakhtar, D., Frampton, J. A., & Wright, H. (1996).
962 *Kearney foundation special report: Background Concentrations of Trace and Major Elements in*
963 *California Soils*. Kearney Foundation of Soil Science, Division of Agriculture and Natural
964 Resources, University of California.
965 Brahney, J., Mahowald, N., Ward, D. S., Ballantyne, A. P., & Neff, J. C. (2015). Is atmospheric
966 phosphorus pollution altering global alpine Lake stoichiometry? *Global Biogeochemical Cycles*,
967 *29*(9), 1369–1383. https://doi.org/10.1002/2015GB005137
968 Browning, T. J., Achterberg, E. P., Engel, A., & Mawji, E. (2021). Manganese co-limitation of
969 phytoplankton growth and major nutrient drawdown in the Southern Ocean. *Nature*
970 *Communications*, *12*(1), 884. https://doi.org/10.1038/s41467-021-21122-6

971 Buccolieri, A., Buccolieri, G., Dell'Atti, A., Strisciullo, G., & Gagliano-Candela, R. (2010).
972 Monitoring of total and bioavailable heavy metals concentration in agricultural soils.
973 *Environmental Monitoring and Assessment*, *168*(1), 547–560. https://doi.org/10.1007/s10661-
974 009-1133-0
975 Bullard, J., Baddock, M., McTainsh, G., & Leys, J. (2008). Sub-basin scale dust source
976 geomorphology detected using MODIS. *Geophysical Research Letters*, *35*(15), L15404.
977 https://doi.org/10.1029/2008GL033928
978 Burrows, S. M., Elbert, W., Lawrence, M. G., & Poschl, U. (2009). Bacteria in the global
979 atmosphere--Part 1: Review and synthesis of literature for different ecosystems. *Atmospheric*
980 *Chemistry and Physics*, *9*, 9263–9280.
981 Burt, R., Weber, T., Park, S., Yochum, S., & Ferguson, R. (2011). Trace Element Concentration
982 and Speciation in Selected Mining-Contaminated Soils and Water in Willow Creek Floodplain,
983 Colorado. *Applied and Environmental Soil Science*, *2011*, 237071.
984 https://doi.org/10.1155/2011/237071
985 Cabrera, F., Clemente, L., Barrientos, E. D., Lopez, R., & Murillo, J. (1999). Heavy metal
986 pollution of soils affected by the Guadiamar toxic flood. *Science of the Total Environemnt*,
987 *242*(1–3), 117–129. https://doi.org/10.1016/S0048-9697(99)00379-4
988 Cancela, R. C., de Abreu, C. A., & Paz-Gonzalez, A. (2002). DTPA and Mehlich-3
989 micronutrient extractability in natural soils. *Communications in Soil Science and Plant Analysis*,
990 *33*(15–18), 2879–2893. https://doi.org/10.1081/CSS-120014488
991 Canfield, D. E., Kristensen, E., & Thamdrup, B. (2005). The Iron and Manganese Cycles. In
992 *Advances in Marine Biology*, *48* (pp. 269–312). Elsevier. https://doi.org/10.1016/S0065-
993 2881(05)48008-6

994 Cassol, J. C., Pletsch, A. L., Costa Júnior, I. L., Bocardi, J., Alovisil, A. M. T., & Fronza, F. L.
995 (2020). Natural contents of metals in soils from basaltic origins in western Parana, Brazil.
996 *Revista Brasileira de Ciências Agrárias*, *15*(2). https://doi.org/10.5039/agraria.v15i2a6992
997 Cavallari, J. M., Eisen, E. A., Fang, S. C., Schwartz, J., Hauser, R., Herrick, R. F., & Christiani,
998 D. C. (2008). PM2.5 metal exposures and nocturnal heart rate variability: A panel study of
999 boilermaker construction workers. *Environmental Health: A Global Access Science Source*, *7*.
1000 https://doi.org/10.1186/1476-069X-7-36
1001 Chen, J. S., Wei, F. S., Zheng, C. J., Wu, Y. Y., & Adriano, D. C. (1991). Background
1002 concentrations of elements in soils of China. *Water Air and Soil Pollution*, *57*(8), 699–712.
1003 https://doi.org/10.1007/BF00282934
1004 Chen, M., Ma, L. Q., & Harris, W. G. (1999). Baseline concentrations of 15 trace elements in
1005 Florida surface soils. *Journal of Environmental Quality*, *28*(4), 1173–1181.
1006 https://doi.org/10.2134/jeq1999.00472425002800040018x
1007 Chen, M., Ma, L. Q., & Li, Y. C. (2000). Concentrations of P, K, Al, Fe, Mn, Cu, Zn, and As in
1008 marl soils from south Florida. *Annual Proceedings Soil and Crop Science Society of Florida*, *59*,
1009 124–129.
1010 China, S., Veghte, D., Ahkami, A. H., Weis, J., Jansson, C., Guenther, A. B., Gilles, M. K., &
1011 Laskin, A. (2020). Microanalysis of Primary Biological Particles from Model Grass over Its Life
1012 Cycle. *ACS Earth and Space Chemistry*, *4*(10), 1895–1905.
1013 https://doi.org/10.1021/acsearthspacechem.0c00144
1014 Computational and Information Systems Laboratory (2019). Cheyenne: HPE/SGI ICE XA
1015 System (NCAR Community Computing). Boulder, CO: National Center for Atmospheric
1016 Research. Retrieved from https://doi.org/10.5065/D6RX99HX

1017 Córdoba, P., Ochoa-Gonzalez, R., Font, O., Izquierdo, M., Querol, X., Leiva, C., López-Antón,
1018 M. A., Díaz-Somoano, M., Rosa Martinez-Tarazona, M., Fernandez, C., & Tomás, A. (2012).
1019 Partitioning of trace inorganic elements in a coal-fired power plant equipped with a wet Flue Gas
1020 Desulphurisation system. *Fuel*, *92*(1), 145–157. https://doi.org/10.1016/j.fuel.2011.07.025
1021 da Silva Costa, R. D., Paula Neto, P., Costa Campos, M. C., do Nascimento, W. B., do
1022 Nascimento, C. W., Silva, L. S., & da Cunha, J. M. (2017). Natural contents of heavy metals in
1023 soils of the southern Amazonas state, Brazil. *Semina-Ciencias Agrarias*, *38*(6), 3499–3513.
1024 https://doi.org/10.5433/1679-0359.2017v38n6p3499
1025 da Silva, Y. J. A. B., do Nascimento, C. W. A., Cantalice, J. R. B., da Silva, Y. J. A. B., & Cruz,
1026 C. M. C. A. (2015). Watershed-scale assessment of background concentrations and guidance
1027 values for heavy metals in soils from a semiarid and coastal zone of Brazil. *Environmental*
1028 *Monitoring and Assessment*, *187*(9), 558. https://doi.org/10.1007/s10661-015-4782-1
1029 Dantu, S. (2010a). Factor analysis applied to a geochemical study of soils from parts of Medak
1030 and Sangareddy areas, Medak district, Andhra Pradesh, India. *Environmental Monitoring and*
1031 *Assessment*, *162*(1–4), 139–152. https://doi.org/10.1007/s10661-009-0782-3
1032 Dantu, S. (2010b). Geochemical patterns in soils in and around Siddipet, Medak District, Andhra
1033 Pradesh, India. *Environmental Monitoring and Assessment*, *170*(1–4), 681–701.
1034 https://doi.org/10.1007/s10661-009-1267-0
1035 Darwish, M. A. G., & Poellmann, H. (2015). Trace elements assessment in agricultural and
1036 desert soils of Aswan area, south Egypt: Geochemical characteristics and environmental impacts.
1037 *Journal of African Earth Sciences*, *112*(A), 358–373.
1038 https://doi.org/10.1016/j.jafrearsci.2015.06.018

1039 Davey, M. P., Berg, B., Emmett, B. A., & Rowland, P. (2007). Decomposition of oak leaf litter
1040 is related to initial litter Mn concentrations. *Canadian Journal of Botany*, *85*(1), 16–24.
1041 https://doi.org/10.1139/b06-150
1042 Davies-Barnard, T., & Friedlingstein, P. (2020). The Global Distribution of Biological Nitrogen
1043 Fixation in Terrestrial Natural Ecosystems. *Global Biogeochemical Cycles*, *34*(3).
1044 https://doi.org/10.1029/2019GB006387
1045 Davison, R. L., Natusch, D. F. S., Wallace, J. R., & Evans, C. A. (1974). Trace elements in fly
1046 ash. Dependence of concentration on particle size. *Environmental Science & Technology*, *8*(13),
1047 1107–1113. https://doi.org/10.1021/es60098a003
1048 de Souza, C. A. C. de, Machado, A. T., Lima, L. R. P. de A., & Cardoso, R. J. C. (2010).
1049 Stabilization of electric-arc furnace dust in concrete. *Materials Research*, *13*(4), 513–519.
1050 https://doi.org/10.1590/S1516-14392010000400014
1051 de Souza, J. J., Pereira Abrahao, W. A., de Mello, J. W., da Silva, J., da Costa, L. M., & de
1052 Oliveira, T. S. (2015). Geochemistry and spatial variability of metal(loid) concentrations in soils
1053 of the state of Minas Gerais, Brazil. *Science of the Total Environment*, *505*, 338–349.
1054 https://doi.org/10.1016/j.scitotenv.2014.09.098
1055 Dentener, F., Drevet, J., Lamarque, J. F., Bey, I., Eickhout, B., Fiore, A. M., Hauglustaine, D.,
1056 Horowitz, L. W., Krol, M., Kulshrestha, U. C., Lawrence, M., Galy-Lacaux, C., Rast, S.,
1057 Shindell, D., Stevenson, D., Van Noije, T., Atherton, C., Bell, N., Bergman, D., . . . Wild, O.
1058 (2006). Nitrogen and sulfur deposition on regional and global scales: A multimodel evaluation.
1059 *Global Biogeochemical Cycles*, *20*(4). https://doi.org/10.1029/2005GB002672

1060 Desboeufs, K. v., Sofikitis, A., Losno, R., Colin, J. L., & Ausset, P. (2005). Dissolution and
1061 solubility of trace metals from natural and anthropogenic aerosol particulate matter.
1062 *Chemosphere*, *58*(2), 195–203. https://doi.org/10.1016/j.chemosphere.2004.02.025
1063 Després, VivianeR., Huffman, J. A., Burrows, S. M., Hoose, C., Safatov, AleksandrS., Buryak,
1064 G., Fröhlich-Nowoisky, J., Elbert, W., Andreae, MeinratO., Pöschl, U., & Jaenicke, R. (2012).
1065 Primary biological aerosol particles in the atmosphere: a review. *Tellus B: Chemical and*
1066 *Physical Meteorology*, *64*(1), 15598. https://doi.org/10.3402/tellusb.v64i0.15598
1067 do Nascimento, C. W., Vieira Lima Luiz Henrique and da Silva, F. L., Biondi, C. M., & Costa
1068 Campos, M. C. (2018). Natural concentrations and reference values of heavy metals in
1069 sedimentary soils in the Brazilian Amazon. *Environmental Monitoring and Assessment*, *190*(10).
1070 https://doi.org/10.1007/s10661-018-6989-4
1071 Dolan, R., Vanloon, J., Templeton, D., & Paudyn, A. (1990). Assessment of ICP-MS for routine
1072 multielement analysis of soil samples in environmental trace-element studies. *Fresenius Journal*
1073 *of Analytical Chemistry*, *336*(2), 99–105. https://doi.org/10.1007/BF00322545
1074 Dreher, K. L., Jaskot, R. H., Lehmann, J. R., Richards, J. H., McGee, J. K., Ghio, A. J., & Costa,
1075 D. L. (1997). Soluble transition metals mediate residual oil fly ash induced acute lung injury.
1076 *Journal of Toxicology and Environmental Health*, *50*(3), 285–305.
1077 https://doi.org/10.1080/009841097160492
1078 Expósito, A., Markiv, B., Ruiz-Azcona, L., Santibáñez, M., & Fernández-Olmo, I. (2021).
1079 Personal inhalation exposure to manganese and other trace metals in an environmentally exposed
1080 population: Bioaccessibility in size-segregated particulate matter samples. *Atmospheric Pollution*
1081 *Research*, *12*(8). https://doi.org/10.1016/j.apr.2021.101123

1082 Fernandes, A. R., de Souza, E. S., de Souza Braz, A. M., Birani, S. M., & Alleoni, L. R. F.
1083 (2018). Quality reference values and background concentrations of potentially toxic elements in
1084 soils from the Eastern Amazon, Brazil. *Journal of Geochemical Exploration*, *190*, 453–463.
1085 https://doi.org/10.1016/j.gexplo.2018.04.012
1086 Foulds, W. (1993). Nutrient concentrations of Foliage and soil in south-western Australia. *New*
1087 *Phytologist*, *125*(3), 529–546. https://doi.org/10.1111/j.1469-8137.1993.tb03901.x
1088 Franklin, R. E., Duis, L., Smith, B. R., Brown, R., & Toler, J. E. (2003). Elemental
1089 concentrations in soils of South Carolina. *Soil Science*, *168*(4), 280–291.
1090 https://doi.org/10.1097/00010694-200304000-00005
1091 Frey, S. D., Ollinger, S., Nadelhoffer, K., Bowden, R., Brzostek, E., Burton, A., Caldwell, B. A.,
1092 Crow, S., Goodale, C. L., Grandy, A. S., Finzi, A., Kramer, M. G., Lajtha, K., LeMoine, J.,
1093 Martin, M., McDowell, W. H., Minocha, R., Sadowsky, J. J., Templer, P. H., & Wickings, K.
1094 (2014). Chronic nitrogen additions suppress decomposition and sequester soil carbon in
1095 temperate forests. *Biogeochemistry*, *121*(2), 305–316. https://doi.org/10.1007/s10533-014-0004-
1096 0
1097 Galloway, J. N., Winiwarter, W., Leip, A., Leach, A. M., Bleeker, A., & Erisman, J. W. (2014).
1098 Nitrogen footprints: past, present and future. *Environmental Research Letters*, *9*(11).
1099 https://doi.org/https://doi.org/10.1088/1748-9326/9/11/115003
1100 Gelaro, R., McCarty, W., Suárez, M. J., Todling, R., Molod, A., Takacs, L., Randles, C.,
1101 Darmenov, A., Bosilovich, M. G., Reichle, R., Wargan, K., Coy, L., Cullather, R., Draper, C.,
1102 Akella, S., Buchard, V., Conaty, A., da Silva, A., Gu, W., . . . & Zhao, B. (2017). The modern-
1103 era retrospective analysis for research and applications, version 2 (MERRA-2). *Journal of*
1104 *Climate*, *30*(13), 5419-5454. https://doi.org/10.1175/JCLI-D-16-0758.1

1105 Ghaemi, Z., Karbassi, A. R., Moattar, F., Hassani, A., & Khorasani, N. (2015). Evaluating soil
1106 metallic pollution and consequent human health hazards in the vicinity of an industrialized zone,
1107 case study of Mubarakeh steel complex, Iran. *Journal of Environmental Health Science and*
1108 *Engineering*, *13*. https://doi.org/10.1186/s40201-015-0231-x
1109 Ginoux, P., Prospero, J., Gill, T. E., Hsu, N. C., & Zhao, M. (2012). Global scale attribution of
1110 anthropogenic and natural dust sources and their emission rates based on MODIS deep blue
1111 aerosol products. *Reviews of Geophysics*, *50*(RG3005). https://doi.org/10.1029/2012RG000388
1112 Hamilton, D. S., Perron, M. M. G., Bond, T. C., Bowie, A. R., Buchholz, R. R., Guieu, C., Ito,
1113 A., Maenhaut, W., Myriokefalitakis, S., Olgun, N., Rathod, S. D., Schepanski, K., Tagliabue, A.,
1114 Wagner, R., & Mahowald, N. M. (2022). Earth, Wind, Fire, and Pollution: Aerosol Nutrient
1115 Sources and Impacts on Ocean Biogeochemistry. *Annual Review of Marine Science*, *14*(1), 303–
1116 330. https://doi.org/10.1146/annurev-marine-031921-013612
1117 Hand, J. L., Gill, T. E., & Schichtel, B. A. (2017). Spatial and seasonal variability in fine mineral
1118 dust and coarse aerosol mass at remote sites across the United States. *Journal of Geophysical*
1119 *Research*, *122*(5), 3080–3097. https://doi.org/10.1002/2016JD026290
1120 Hand, J. L., Gill, T. E., & Schichtel, B. A. (2019). Urban and rural coarse aerosol mass across the
1121 United States: Spatial and seasonal variability and long-term trends. *Atmospheric Environment*,
1122 *218*. https://doi.org/10.1016/j.atmosenv.2019.117025
1123 Hansen, H. K., Pedersen, A. J., Ottosen, L. M., & Villumsen, A. (2001). Speciation and mobility
1124 of cadmium in straw and wood combustion fly ash. *Chemosphere*, *45*(1), 123–128.
1125 https://doi.org/10.1016/S0045-6535(01)00026-1
1126 Hansen, M. C., Potapov, P. v, Moore, R., Hancher, M., Turubanova, S. A., Tyukavina, A., Thau,
1127 D., Stehman, S. v, Goetz, S. J., Loveland, T. R., Kommareddy, A., Egorov, A., Chini, L., Justice,

C. O., & Townshend, J. R. G. (2013). High-Resolution Global Maps of 21st-Century Forest Cover Change. *Science*, *342*(6160), 850–853. https://doi.org/10.1126/science.1244693

Hartley, I. P., Hill, T. C., Chadburn, S. E., & Hugelius, G. (2021). Temperature effects on carbon storage are controlled by soil stabilisation capacities. *Nature Communications*, *12*(1), 6713. https://doi.org/10.1038/s41467-021-27101-1

Haynes, R. J., & Swift, R. S. (1991). Concentrations of extractable Cu, Zn, Fe and Mn in a group of soils as influenced by air-drying and oven-drying and rewetting. *Geoderma*, *49*(3–4), 319–333. https://doi.org/10.1016/0016-7061(91)90083-6

He, Q., & Walling, D. E. (1997). The distribution of fallout ^{137}Cs and ^{210}Pb in undisturbed and cultivated soils. *Applied Radiation and Isotopes*, *48*(5), 677–690. https://doi.org/10.1016/S0969-8043(96)00302-8

Heald, C., & Spracklen, D. (2009). Atmospheric budget of primary biological aerosol particles from fungal sources. *Geophysical Research Letters*, *36*(9), L09806. https://doi.org/10.1029/2009GL037493

Hertel, O., Geels, C., Frohn, L. M., Ellermann, T., Skjøth, C.A., Løfstrøm, P., Christensen, J. H., Andersen, H. V., & Peel, R. G. (2013). Assessing atmospheric nitrogen deposition to natural and semi-natural ecosystems – Experience from Danish studies using the DAMOS. *Atmospheric Environment*, *66*, 151-160. https://doi.org/10.1016/j.atmosenv.2012.02.071

Hofrichter, M. (2002). Review: lignin conversion by manganese peroxidase (MnP). *Enzyme and Microbial Technology*, *30*(4), 454-466. https://doi.org/10.1016/S0141-0229(01)00528-2

Hsu, C. Y., Chiang, H. C., Lin, S. L., Chen, M. J., Lin, T. Y., & Chen, Y. C. (2016). Elemental characterization and source apportionment of PM10 and PM2.5 in the western coastal area of

central Taiwan. *Science of the Total Environment*, *541*, 1139–1150. https://doi.org/10.1016/j.scitotenv.2015.09.122

Hua, Z., Chun-ming, J., Yong-gang, X., & Qiang, M. (2013). Analysis on Concentration, Distribution and Budgets of Mn and Zn in Soybean by Using ICP-AES. *Spectroscopy and Spectral Analysis*, *33*(4), 1112–1115. https://doi.org/10.3964/j.issn.1000-0593(2013)04-1112-04

Huffman, G. P., Huggins, F. E., Shah, N., Huggins, R., Linak, W. P., Miller, C. A., Pugmire, R. J., Meuzelaar, H. L. C., Seehra, M. S., & Manivannan, A. (2000). Characterization of Fine Particulate Matter Produced by Combustion of Residual Fuel Oil. *Journal of the Air & Waste Management Association*, *50*(7), 1106–1114. https://doi.org/10.1080/10473289.2000.10464157

Hurrell, J. W., Holland, M. M., Gent, P. R., Chan, S., Kay, J. E., Kushner, P. J., Lamarque, J.-F., Large, W. G., Lawrence, D., Lindsay, K., Lipscomb, W. H., Long, M. C., Mahowald, N., Marsh, D. R., Neale, R. B., Rasch, P., Vavrus, S., Vertenstein, M., Bader, D., Collins, W. D., Hack, J. J., Kiehl, J., & Marshall, S. (2013). The Community Earth System Model: A Framework for Collaborative Research. *Bulletin of the American Meteorological Society*, *94*(9), 1339-1360. https://doi.org/10.1175/BAMS-D-12-00121.1

Hurtt, G. C., Chini, L. P., Frolking, S., Betts, R. A., Feddema, J., Fischer, G., Fisk, J. P., Hibbard, K., Houghton, R. A., Janetos, A., Jones, C. D., Kindermann, G., Kinoshita, T., Goldewijk, K. K., Riahi, K., Shevliakova, E., Smith, S., Stehfest, E., Thomson, A., . . . Wang, Y. P. (2011). Harmonization of land-use scenarios for the period 1500-2100: 600 years of global gridded annual land-use transitions, wood harvest, and resulting secondary lands. *Climatic Change*, *109*(1–2), 117–161. https://doi.org/10.1007/s10584-011-0153-2

1171 Ikem, A., Campbell, M., Nyirakabibi, I., & Garth, J. (2008). Baseline concentrations of trace
1172 elements in residential soils from Southeastern Missouri. *Environmental Monitoring and*
1173 *Assessment*, *140*(1), 69–81. https://doi.org/10.1007/s10661-007-9848-2
1174 Imran, M., Khan, A.-H., Aziz-ul-Hassan, Kanwal, F., Mitu, L., Amir, M., & Iqbal, M. A. (2010).
1175 Evaluation of Physico-Chemical Characteristics of Soil Samples Collected from Harrapa-
1176 Sahiwal (Pakistan). *Asian Journal of Chemistry*, *22*(6), 4823–4830.
1177 Iñigo, V., Andrades, M., Alonso-Martirena, J. I., Marín, A., & Jiménez-Ballesta, R. (2011).
1178 Multivariate Statistical and GIS-Based Approach for the Identification of Mn and Ni
1179 Concentrations and Spatial Variability in Soils of a Humid Mediterranean Environment: La
1180 Rioja, Spain. *Water, Air, & Soil Pollution*, *222*(1), 271–284. https://doi.org/10.1007/s11270-011-
1181 0822-9
1182 IPCC, (2000). *Special Report on Land Use, Land-Use Change, and Forestry*. Cambridge
1183 University Press. https://www.ipcc.ch/report/land-use-land-use-change-and-forestry
1184 Ivezic, V., Singh, B. R., Almas, A. R., & Loncaric, Z. (2011). Water extractable concentrations
1185 of Fe, Mn, Ni, Co, Mo, Pb and Cd under different land uses of Danube basin in Croatia. *Acta*
1186 *Agriculturae Scandinavica, Section B — Soil & Plant Science*, *61*(8), 747–759.
1187 https://doi.org/10.1080/09064710.2011.557392
1188 Jahiruddin, M., Harada, H., Hatanaka, T., & Islam, M. R. (2000). Status of trace elements in
1189 agricultural soils of Bangladesh and relationship with soil properties. *Soil Science and Plant*
1190 *Nutrition*, *46*(4), 963–968. https://doi.org/10.1080/00380768.2000.10409161
1191 Jang, H. N., Seo, Y. C., Lee, J. H., Hwang, K. W., Yoo, J. I., Sok, C. H., & Kim, S. H. (2007).
1192 Formation of fine particles enriched by V and Ni from heavy oil combustion: Anthropogenic

1193 sources and drop-tube furnace experiments. *Atmospheric Environment*, *41*(5), 1053–1063.
1194 https://doi.org/10.1016/j.atmosenv.2006.09.011
1195 Jones, M. E., LaCroix, R. E., Zeigler, J., Ying, S. C., Nico, P. S., & Keiluweit, M. (2020).
1196 Enzymes, Manganese, or Iron? Drivers of Oxidative Organic Matter Decomposition in Soils.
1197 *Environmental Science and Technology*, *54*(21), 14114−14123.
1198 Joshi, D., Srivastava, P. C., Dwivedi, R., Pachauri, S. P., & Shukla, A. K. (2017). Chemical
1199 Fractions of Mn in Acidic Soils and Selection of Suitable Soil Extractants for Assessing Mn
1200 Availability to Maize (Zea Mays L.). *Communications in Soil Science and Plant Analysis*, *48*(8),
1201 886–897. https://doi.org/10.1080/00103624.2017.1322601
1202 Kanakidou, M., Myriokefalitakis, S., Daskalakis, N., Fanourgakis, G., Nenes, A., Baker, A. R.,
1203 Tsigaridis, K., & Mihalopoulos, N. (2016). Past, present, and future atmospheric nitrogen
1204 deposition. *Journal of the Atmospheric Sciences*, *73*(5), 2039–2047. https://doi.org/10.1175/JAS-
1205 D-15-0278.1
1206 Kassaye, Y. A., Skipperud, L., Meland, S., Dadebo, E., Einset, J., & Salbu, B. (2012). Trace
1207 element mobility and transfer to vegetation within the Ethiopian Rift Valley lake areas. *Journal*
1208 *of Environmental Monitoring*, *14*(10), 2698–2709. https://doi.org/10.1039/c2em30271c
1209 Kaste, J. M., Friedland, A. J., & Stürup, S. (2003). Using stable and radioactive isotopes to trace
1210 atmospherically deposited Pb in Montane forest soils. *Environmental Science & Technology*,
1211 *37*(16), 3560–3567. https://doi.org/10.1021/es026372k
1212 Kauffman, J., Cummings, D. L., Ward, D. E., Babbitt, R. (1995). Fire in the Brazilian Amazon:
1213 1. Biomass, nutrient pools, and losses in slashed primary forests. *Oecologia*, *104*, 397-408.
1214 https://doi.org/10.1007/BF00341336

1215 Keiluweit, M., Nico, P., Harmon, M. E., Mao, J., Pett-Ridge, J., & Kleber, M. (2015). Long-term
1216 litter decomposition controlled by manganese redox cycling. *Proceedings of the National*
1217 *Academy of Sciences of the United States of America*, *112*(38), E5253–E5260.
1218 https://doi.org/10.1073/pnas.1508945112
1219 Kellogg, C. A., & Griffin, D. W. (2006). Aerobiology and the global transport of desert dust.
1220 *Trends in Ecology and Evolution*, *21*(11), 638-644. https://doi.org/10.1016/j.tree.2006.07.004
1221 Kloss, S., Zehetner, F., Oburger, E., Buecker Jannis and Kitzler, B., Wenzel, W. W., Wimmer,
1222 B., & Soja, G. (2014). Trace element concentrations in leachates and mustard plant tissue
1223 (Sinapis alba L.) after biochar application to temperate soils. *Science of the Total Environment*,
1224 *481*, 498–508. https://doi.org/10.1016/j.scitotenv.2014.02.093
1225 Kok, J. F., Mahowald, N. M., Fratini, G., Gillies, J. A., Ishizuka, M., Leys, J. F., Mikami, M.,
1226 Park, M.-S., Park, S.-U., Van Pelt, R. S., & Zobeck, T. M. (2014a). An improved dust emission
1227 model – Part 1: Model description and comparison against measurements. *Atmospheric*
1228 *Chemistry and Physics*, *14*, 13023–13041. https://doi.org/10.5194/acp14-13023-2014.
1229 Kok, J. F., Albani, S., Mahowald, N. M., & Ward, D. S. (2014b). An improved dust emission
1230 model – Part 2: Evaluation in the Community Earth System Model, with implications for the use
1231 of dust source functions, *Atmospheric Chemistry and Physics*, *14*, 13043–13061.
1232 https://doi.org/10.5194/acp-14-13043-2014
1233 Koukouzas, N., Hämäläinen, J., Papanikolaou, D., Tourunen, A., & Jäntti, T. (2007).
1234 Mineralogical and elemental composition of fly ash from pilot scale fluidised bed combustion of
1235 lignite, bituminous coal, wood chips and their blends. *Fuel*, *86*(14), 2186–2193.
1236 https://doi.org/10.1016/j.fuel.2007.03.036

1237 Kranabetter, J. M., Philpott, T. J., & Dunn, D. E. (2021). Manganese limitations and the
1238 enhanced soil carbon sequestration of temperate rainforests. *Biogeochemistry*, *156*(2), 195–209.
1239 https://doi.org/10.1007/s10533-021-00840-5
1240 Krawchuk, M. A., Moritz, M. A., Parisien, M. A., Van Dorn, J., & Hayhoe, K. (2009). Global
1241 Pyrogeography: the Current and Future Distribution of Wildfire. *PLOS ONE*, *4*(4): e5102.
1242 https://doi.org/10.1371/journal.pone.0005102
1243 Kuss, J., & Kremling, K. (1999). Spatial variability of particle associated trace elements in near-
1244 surface waters of the North Atlantic (30°N/60°W to 60°N/2°W), derived by large volume
1245 sampling. *Marine Chemistry*, *68*(1-2), 71-86. https://doi.org/10.1016/S0304-4203(99)00066-3
1246 Lavado, R. S., & Porcelli, C. A. (2000). Contents and main fractions of trace elements in Typic
1247 Argiudolls of the Argentinean Pampas. *Chemical Speciation and Bioavailability*, *12*(2), 67–70.
1248 https://doi.org/10.3184/095422900782775553
1249 Lawrence, D. M., Fisher, R. A., Koven, C. D., Oleson, K. W., Swenson, S. C., Bonan, G.,
1250 Collier, N., Ghimire, B., van Kampenhout, L., Kennedy, D., Kluzek, E., Lawrence, P. J., Li, F.,
1251 Li, H., Lombardozzi, D., Riley, W. J., Sacks, W. J., Shi, M., Vertenstein, M., . . . Zeng, X.
1252 (2019). The Community Land Model Version 5: Description of New Features, Benchmarking,
1253 and Impact of Forcing Uncertainty. *Journal of Advances in Modeling Earth Systems*, *11*(12),
1254 4245–4287. https://doi.org/10.1029/2018MS001583
1255 Li., L., Mahowald, N. M., Kok, J. F., Liu, X., Wu, M., Leung, D. M., Hamilton, D. S., Emmons,
1256 L. K., Huang, Y., Sexton, N., & Wan, J. (2022). Importance of different parameterization
1257 changes for the updated dust cycle modeling in the Community Atmosphere Model (version 6.1).
1258 *Geoscientific Model Development*, *15*(22), 8181-8219. https://doi.org/10.5194/gmd-15-8181-
1259 2022

1260 Li, L., Mahowald, N., Miller, R. L., Perez Garcia-Pando, C., Klose, M., Hamilton, D. S.,
1261 Ageitos, M. G., Ginoux, P., Balkanski, Y., Green, R. O., Kalashnikova, O., Kok, J. F., Obiso, V.,
1262 Paynter, D., Thompson, D. R. (2021). Quantifying the range of the dust direct radiative effect
1263 due to source mineralogy uncertainty. *Atmospheric Chemistry and Physics Discussions*, *21*(5),
1264 3973-4005. https://doi.org/10.5194/ acp-2020-547
1265 Linak, W. P., Andrew Miller, C., & Wendt, J. O. L. (2000a). Fine particle emissions from
1266 residual fuel oil combustion: Characterization and mechanisms of formation. *Proceedings of the*
1267 *Combustion Institute*, *28*(2), 2651–2658. https://doi.org/10.1016/S0082-0784(00)80684-0
1268 Linak, W. P., Miller, C. A., & Wendt, J. O. L. (2000b). Comparison of particle size distributions
1269 and elemental partitioning from the combustion of pulverized coal and residual fuel oil. *Journal*
1270 *of the Air & Waste Management Association*, *50*(8), 1532–1544.
1271 https://doi.org/10.1080/10473289.2000.10464171
1272 Lindell, L., Astrom, M., & Oberg, T. (2010). Land-use versus natural controls on soil fertility in
1273 the Subandean Amazon, Peru. *Science of the Total Environment*, *408*(4), 965–975.
1274 https://doi.org/10.1016/j.scitotenv.2009.10.039
1275 Liu, X., Easter, R. C., Ghan, S. J., Zaveri, R., Rasch, P., Shi, X., Lamarque, J.-F., Gettleman, A.,
1276 Morrison, H., Vitt, F., Conley, A., Park, S., Neale, R., Hannay, C., Ekman, A. M. L., Hess, P.,
1277 Mahowald, N. M., Collins, W., Iacoco, M. J., . . . & Mitchell, D. (2011). Toward a minimal
1278 representation of aerosol direct and indirect effects: Model description and evaluation.
1279 *Geoscientific Model Development Discussions*, *4*(4), 3485–3598. https://doi.org/10.5194/gmdd-
1280 4-3485-2011
1281 Liu, X., Ma, P. L., Wang, H., Tilmes, S., Singh, B., Easter, R. C., Ghan, S. J., & Rasch, P. J.
1282 (2016). Description and evaluation of a new four-mode version of the Modal Aerosol Module

(MAM4) within version 5.3 of the Community Atmosphere Model. *Geoscientific Model Development*, *9*(2), 505–522. https://doi.org/10.5194/gmd-9-505-2016

Loosmore, G. A. (2003). Evaluation and development of models for resuspension of aerosols at short times after deposition. *Atmospheric Environment*, *37*(5), 639-647. https://doi.org/10.1016/S1352-2310(02)00902-0

Lv, Y., Kabanda, G., Chen, Y., Wu, C., & Li, W. (2022). Spatial distribution and ecological risk assessment of heavy metals in manganese (Mn) contaminated site. *Frontiers in Environmental Science*, *10*. https://doi.org/10.3389/fenvs.2022.942544

Ma, L. Q., Tan, F., & Harris, W. G. (1997). Concentrations and distributions of eleven metals in Florida soils. *Journal of Environmental Quality*, *26*(3), 769. https://www.proquest.com/scholarly-journals/concentrations-distributions-eleven-metals/docview/197389221/se-2?accountid=10267

Machado, J., Brehm, F., Moraes, C., Santos, C., Vilela, A., & Cunha, J. (2006). Chemical, physical, structural and morphological characterization of the electric arc furnace dust. *Journal of Hazardous Materials*, *136*(3), 953–960. https://doi.org/10.1016/j.jhazmat.2006.01.044

Maenhaut, W., Fernández-Jiménez, M.-T., Rajta, I., & Artaxo, P. (2002). Two-year study of atmospheric aerosols in Alta Floresta, Brazil: Multielemental composition and source apportionment. *Nuclear Instruments and Methods in Physics Research*, B189, 243-248. https://doi.org/10.1016/S0168-583X(01)01050-3

Maenhaut, W., Fernández-Jiménez, M.-T., Rajta, I., Dubtsov I, S., Meixner, F. X., Andreae, M. O., Torr, S., Hargrove, J. W., Chimanga, P., & Mlambo, J. (2000). Long-term aerosol composition measurements and source apportionment at Rukomechi, Zimbabwe. *Journal of Aerosol Science*, *31*, Suppl. 1, S228-S229. https://doi.org/10.1016/S0021-8502(00)90237-4

1306 Maenhaut, W., Fernández-Jiménez, M.-T., & Artaxo, P. (1999). Long-term study of atmospheric
1307 aerosols in Cuiaba, Brazil : multielemental composition, sources and source apportionment.
1308 *Journal of Aerosol Science*, *30*(0021–8502), S259–S260.
1309 Mahowald, N., Albani, S., Kok, J. F., Engelstaeder, S., Scanza, R., Ward, D. S., & Flanner, M.
1310 G. (2014). The size distribution of desert dust aerosols and its impact on the Earth system.
1311 *Aeolian Research*, *15*, 53-71. https://doi.org/10.1016/j.aeolia.2013.09.002
1312 Mahowald, N. M., Artaxo, P., Baker, A. R., Jickells, T. D., Okin, G. S., Randerson, J. T., &
1313 Townsend, A. R. (2005). Impacts of biomass burning emissions and land use change on
1314 Amazonian atmospheric phosphorus cycling and deposition. *Global Biogeochemical Cycles*,
1315 *19*(4). https://doi.org/10.1029/2005GB002541
1316 Mahowald, N. M., Engelstaedter, S., Luo, C., Sealy, A., Artaxo, P., Benitez-Nelson, C., Bonnet,
1317 S., Chen, Y., Chuang, P. Y., Cohen, D. D., Dulac, F., Herut, B., Johansen, A. M., Kubilay, N.,
1318 Losno, R., Maenhaut, W., Paytan, A., Prospero, J. M., Shank, L. M., & Siefert, R. L. (2009).
1319 Atmospheric iron deposition: Global distribution, variability, and human perturbations. *Annual*
1320 *Review of Marine Science*, *1*, 245–278. https://doi.org/10.1146/annurev.marine.010908.163727
1321 Mahowald, N. M., Hamilton, D. S., Mackey, K. R. M., Moore, J. K., Baker, A. R., Scanza, R. A.,
1322 & Zhang, Y. (2018). Aerosol trace metal leaching and impacts on marine microorganisms.
1323 *Nature Communications*, *9*, 2614. https://doi.org/10.1038/s41467-018-04970-7
1324 Mamane, Y., Miller, J. L., & Dzubay, T. G. (1986). Characterization of individual fly ash
1325 particles emitted from coal- and oil-fired power plants. *Atmospheric Environment (1967)*, *20*(11),
1326 2125–2135. https://doi.org/10.1016/0004-6981(86)90306-9

1327 Martinez-Tarazona, M., Palacios, J. M., Martinez-Alonso, A., & Tascon, J. (1990). The
1328 characterization of organomineral components of low-rank coals. *Fuel Processing Technology*,
1329 *25*, 81–87. https://doi.org/10.1016/0378-3820(90)90097-C
1330 Mashi, S. A., Yaro, S. A., & Haiba, A. S. (2004). Cu, Mn, Fe, and Zn levels in soils of Shika
1331 area, Nigeria. *Biomedical and Environmental Sciences*, *17*(4), 426–431.
1332 McKenzie, R. M. (1957). The distribution of trace elements in some South Australian red-brown
1333 earths. *Australian Journal of Agricultural Research*, *8*(3), 246–252.
1334 https://doi.org/10.1071/AR9570246
1335 Meij, R. (1994). Trace element behavior in coal-fired power plants. *Fuel Processing Technology*,
1336 *39*(1–3), 199–217. https://doi.org/10.1016/0378-3820(94)90180-5
1337 Michopoulos, P., Economou, A., & Nikolis, N. (2004). Soil extractable manganese and uptake in
1338 a natural fir stand grown on calcareous soils. *Communications in Soil Science and Plant*
1339 *Analysis*, *35*(1–2), 233–241. https://doi.org/10.1081/CSS-120027646
1340 Michopoulos, P., Farmaki, E., & Thomaidis, N. (2017). Foliar status and factors affecting foliar
1341 and soil chemistry in a natural aleppo pine forest. *Journal of Plant Nutrition*, *40*(10), 1443–1452.
1342 https://doi.org/10.1080/01904167.2016.1269341
1343 Mikkonen, H. G., Clarke, B. O., Dasika, R., Wallis, C. J., & Reichman, S. M. (2017).
1344 Assessment of ambient background concentrations of elements in soil using combined survey
1345 and open-source data. *Science of the Total Environment*, *580*, 1410–1420.
1346 https://doi.org/10.1016/j.scitotenv.2016.12.106
1347 Miko, S., Durn, G., Adamcova, R., Covic, M., Dubikova, M., Skalsky, R., Kapelj, S., & Ottner,
1348 F. (2003). Heavy metal distribution in karst soils from Croatia and Slovakia. *Environmental*
1349 *Geology*, *45*(2), 262–272. https://doi.org/10.1007/s00254-003-0878-y

Moore, J. A. M., Anthony, M. A., Pec, G. J., Trocha, L. K., Trzebny, A., Geyer, K. M., van Diepen, L. T. A., & Frey, S. D. (2021). Fungal community structure and function shifts with atmospheric nitrogen deposition. *Global Change Biology*, *27*(7), 1349–1364. https://doi.org/10.1111/gcb.15444

Moore, O. W., Curti, L., Woulds, C., Bradley, J. A., Babakhani, P., Mills, B. J. W., Homoky, W. B., Xiao, K., Bray, A. W., Fisher, B. J., Kazemian, M., Kaulich, B., Dale, A. W., & Peacock, C. L. (2023). Long-term organic carbon preservation enhanced by iron and manganese. *Nature*. https://doi.org/10.1038/s41586-023-06325-9

Morales Del Mastro, A., Londonio, A., Jimenez Rebagliati, R., Pereyra, M., Dawidowski, L., Gomez, D., & Smichowski, P. (2015). Plasma-based techniques applied to the determination of 17 elements in partitioned top soils. *Microchemical Journal*, *123*, 224–229. https://doi.org/10.1016/j.microc.2015.07.002

Nalovic, L., & Pinta, M. (1969). Recherches sur les éléments traces dans les sols tropicaux: Étude de quelques sols de madagascar. *Geoderma*, *3*, 117–132. https://doi.org/10.1016/0016-7061(69)90008-1

Nanzyo, M., Yamasaki, S.-I., & Honna, T. (2002). Changes in content of trace and ultratrace elements with an increase in noncrystalline materials in volcanic ash soils of Japan. *Clay Science*, *12*(1), 25–32. https://doi.org/10.11362/jcssjclayscience1960.12.25

Natali, S. M., Sañudo-wilhelmy, S. A., & Lerdau, M. T. (2009). Plant and soil mediation of elevated CO2 impacts on trace metals. *Ecosystems*, *12*(5), 715–727. https://doi.org/10.1007/s10021-009-9251-7

1371 Navas, A., & Lindhorfer, H. (2005). Chemical partitioning of Fe, Mn, Zn and Cr in mountain
1372 soils of the Iberian and Pyrenean ranges (NE Spain). *Soil and Sediment Contamination: An*
1373 *International Journal*, *14*(3), 249–259. https://doi.org/10.1080/15320380590928311
1374 Nguyen, B. T., Do, T. K., Tran, T. van, Dang, M. K., Dell, C. J., Luu, P. V., & Vo, Q. T. K.
1375 (2018). High soil Mn and Al, as well as low leaf P concentration, may explain for low natural
1376 rubber productivity on a tropical acid soil in Vietnam. *Journal of Plant Nutrition*, *41*(7), 903–
1377 914. https://doi.org/10.1080/01904167.2018.1431674
1378 Njofang, C., Matschullat, J., Amougou, A., Tchouankoué, J. P., & Heilmeier, H. (2009). Soil and
1379 plant composition in the Noun river catchment basin, Western Cameroon: a contribution to the
1380 development of a biogeochemical baseline. *Environmental Geology*, *56*(7), 1427–1436.
1381 https://doi.org/10.1007/s00254-008-1237-9
1382 Nriagu, J. O. (1989). A global assessment of natural sources of atmospheric trace metals. *Nature*,
1383 *338*, 47–49.
1384 Nygard, T., Steinnes, E., & Royset, O. (2012). Distribution of 32 Elements in Organic Surface
1385 Soils: Contributions from Atmospheric Transport of Pollutants and Natural Sources. *Water, Air,*
1386 *& Soil Pollution*, *223*(2), 699–713. https://doi.org/10.1007/s11270-011-0895-5
1387 O'Dowd, C. D., de Leeuw, G. (2007). Marine aerosol production: a review of the current
1388 knowledge. *Philosophical Transactions of the Royal Society A*, *365*(1856), 1753-1774.
1389 https://doi.org/10.1098/rsta.2007.2043
1390 Okin, G. S., Mahowald, N., Chadwick, O. A., & Artaxo, P. (2004). Impact of desert dust on the
1391 biogeochemistry of phosphorus in terrestrial ecosystems. *Global Biogeochemical Cycles*, *18*(2).
1392 https://doi.org/10.1029/2003GB002145

1393 Pacyna, J. M., & Pacyna, E. G. (2001). An assessment of global and regional emissions of trace
1394 metals to the atmosphere from anthropogenic sources worldwide. *Environmental Reviews*, *9*(4),
1395 269–298. https://doi.org/10.1139/a01-012
1396 Papadopoulos, F., Prochaska, C., Papadopoulos, A., & Eskridge K. and Kalavrouziotis, I. (2009).
1397 Mn and Zn Micronutrients Concentrations in Acidic Soils and Source Identification Using
1398 Multivariate Statistical Methods. *Communications in Soil Science and Plant Analysis*, *40*(15–
1399 16), 2357–2371. https://doi.org/10.1080/00103620903111285
1400 Papastergios, G., Filippidis, A., Fernandez-Turiel, J.-L., Gimeno, D., & Sikalidis, C. (2011).
1401 Surface Soil Geochemistry for Environmental Assessment in Kavala Area, Northern Greece.
1402 *Water, Air, & Soil Pollution*, *216*(1–4), 141–152. https://doi.org/10.1007/s11270-010-0522-x
1403 Parekh, P. P. (1990). *Atmospheric Environment Vot* (Vol. 24, Issue 2).
1404 Patel, K. S., Chikhlekar, S., Ramteke, S., Sahu, B. L., Dahariya, N. S., & Sharma, R. (2015).
1405 Micronutrient Status in Soil of Central India. *American Journal of Plant Sciences*, *06*(19), 3025–
1406 3037. https://doi.org/10.4236/ajps.2015.619297
1407 Paye, H. de S., de Mello, J. W., Pereira Abrahao, W. A., Fernandes Filho, E. I., Pinto Dias, L. C.,
1408 Oliveira Castro, M. L., de Melo, S. B., & Franca, M. M. (2010). REFERENCE QUALITY
1409 VALUES FOR HEAVY METALS IN SOILS FROM ESPIRITO SANTO STATE, BRAZIL.
1410 *REVISTA BRASILEIRA DE CIENCIA DO SOLO*, *34*(6), 2041–2051.
1411 Petroff, A., and Zhang, L. (2010). Development and validation of a size-resolved particle dry
1412 deposition scheme for application in aerosol transport models. *Geoscientific Model Development*,
1413 *3*(2), 753-769. https://doi.org/10.5194/gmd-3-753-2010
1414 Phillips, C. A., Rogers, B. M., Elder, M., Cooperdock, S., Moubarak, M., Randerson, J. T., &
1415 Frumhoff, P. C. (2022). Escalating carbon emissions from North American boreal forest

1416 wildfires and the climate mitigation potential of fire management. *Science Advances*, *8*(17),
1417 eabl7161. https://doi.org/10.1126/sciadv.abl7161
1418 Poggio, L., de Sousa, L. M., Batjes, N. H., Heuvelink, G. B. M., Kempen, B., Ribeiro, E., and
1419 Rossiter, D.: SoilGrids 2.0 (2021). Producing soil information for the globe with quantified
1420 spatial uncertainty, *SOIL*, *7*, 217–240. https://doi.org/10.5194/soil-7-217-2021
1421 Preda, M., & Cox, M. E. (2002). Trace metal occurrence and distribution in sediments and
1422 mangroves, Pumicestone region, southeast Queensland, Australia. *Environmental International*,
1423 *28*(5), 433–449. https://doi.org/10.1016/S0160-4120(02)00074-0
1424 Prospero, J. M., Barrett, K., Church, T., Dentener, F., Duce, R. A., Galloway, J. N., Levy, H.,
1425 Moody, J., & Quinn, P. (1996). Atmospheric deposition of nutrients to the North Atlantic Basin.
1426 *Biogeochemistry*, *35*(1), 27–73. https://doi.org/10.1007/BF02179824
1427 Puchelt, H., Kramar, U., Cumming, G. L., Krstic, D., Nöltner, Th., Schöttle, M., & Schweikle, V.
1428 (1993). Anthropogenic Pb contamination of soils, southwest Germany. *Applied Geochemistry*, *8*,
1429 71–73. https://doi.org/10.1016/S0883-2927(09)80014-0
1430 Querol, X., Fernández-Turiel, J., & López-Soler, A. (1995). Trace elements in coal and their
1431 behaviour during combustion in a large power station. *Fuel*, *74*(3), 331–343.
1432 https://doi.org/10.1016/0016-2361(95)93464-O
1433 Rashed, M. N. (2010). Monitoring of contaminated toxic and heavy metals, from mine tailings
1434 through age accumulation, in soil and some wild plants at Southeast Egypt. *Journal of*
1435 *Hazardous Materials*, *178*(1–3), 739–746. https://doi.org/10.1016/j.jhazmat.2010.01.147
1436 Rathod, S. D., Hamilton, D. S., Mahowald, N. M., Klimont, Z., Corbett, J. J., & Bond, T. C.
1437 (2020). A mineralogy-based anthropogenic combustion-iron emission Inventory. *Journal of*
1438 *Geophysical Research: Atmospheres*, *125*(17). https://doi.org/10.1029/2019JD032114

1439 Rauch, J. N., & Pacyna, J. M. (2009). Earth's global Ag, Al, Cr, Cu, Fe, Ni, Pb, and Zn cycles.
1440 *Global Biogeochemical Cycles*, *23*(2). https://doi.org/10.1029/2008GB003376
1441 Rekasi, M., & Filep, T. (2012). Fractions and background concentrations of potentially toxic
1442 elements in Hungarian surface soils. *Environmental Monitoring and Assessment*, *184*(12), 7461–
1443 7471. https://doi.org/10.1007/s10661-011-2513-9
1444 Richards, J. R., Schroder, J. L., Zhang, H., Basta, N. T., Wang, Y., & Payton, M. E. (2012).
1445 Trace Elements in Benchmark Soils of Oklahoma. *Soil Science Society of America Journal*,
1446 *76*(6), 2031–2040. https://doi.org/10.2136/sssaj2012.0100
1447 Ridley, D. A., Heald, C. L., & Ford, B. (2012). North African dust export and deposition: A
1448 satellite and model perspective. *Journal of Geophysical Research Atmospheres*, *117*(2).
1449 https://doi.org/10.1029/2011JD016794
1450 Ridley, D. A., Heald, C. L., Kok, J. F., & Zhao, C. (2016). An observationally constrained
1451 estimate of global dust aerosol optical depth. *Atmospheric Chemistry and Physics*, *16*, 15097–
1452 15117. https://doi.org/10.5194/acp-16-15097-2016
1453 Roca, N., Susana Pazos, M., & Bech, J. (2012). Background levels of potentially toxic elements
1454 in soils: A case study in Catamarca (a semiarid region in Argentina). *Catena*, *92*, 55–66.
1455 https://doi.org/10.1016/j.catena.2011.11.009
1456 Roca-Perez, L., Boluda, R., & Perez-Bermudez, P. (2004). Soil-plant relationships, micronutrient
1457 contents, and cardenolide production in natural populations of Digitalis obscura. *Journal of Plant*
1458 *Nutrition and Soil Science*, *167*(1), 79–84. https://doi.org/10.1002/jpln.200320336
1459 Roca-Perez, L., Gil, C., Cervera, M. L., Gonzalvez, A., Ramos-Miras, J., Pons, V., Bech, J., &
1460 Boluda, R. (2010). Selenium and heavy metals content in some Mediterranean soils. *Journal of*
1461 *Geochemical Exploration*, *107*(2, SI), 110–116. https://doi.org/10.1016/j.gexplo.2010.08.004

1462 Rodríguez, S., Calzolai, G., Chiari, M., Nava, S., García, M. I., López-Solano, J., Marrero, C.,
1463 López-Darias, J., Cuevas, E., Alonso-Pérez, S., Prats, N., Amato, F., Lucarelli, F., & Querol, X.
1464 (2020). Rapid changes of dust geochemistry in the Saharan Air Layer linked to sources and
1465 meteorology. *Atmospheric Environment*, *223*, 117186.
1466 https://doi.org/10.1016/j.atmosenv.2019.117186
1467 Rosswall, T. (1976). The internal nitrogen cycle between microorganisms, vegetation and soil.
1468 *Ecological Bulletins*, *22*, 157–167. http://www.jstor.org/stable/20112525
1469 Rusjan, D., Strlic, M., Pucko, D., Selih, V. S., & Korosec-Koruza, Z. (2006). Vineyard soil
1470 characteristics related to content of transition metals in a sub-Mediterranean winegrowing region
1471 of Slovenia. *Geoderma*, *136*(3–4), 930–936. https://doi.org/10.1016/j.geoderma.2006.06.014
1472 Ryder, C. L., Highwood, E. J., Walser, A., Seibert, P., Philipp, A., & Weinzierl, B. (2019).
1473 Coarse and giant particles are ubiquitous in Saharan dust export regions and are radiatively
1474 significant over the Sahara. *Atmospheric Chemistry and Physics*, *19*, 15353-15376.
1475 https://doi.org/10.5194/acp-19-15353-2019
1476 Saglam, C. (2017). Heavy metal concentrations in serpentine soils and plants from Kizildag
1477 National Park (Isparta) in Turkey. *Fresenius Environmental Bulletin*, *26*(6), 3995–4003.
1478 Sako, A., Mills, A. J., & Roychoudhury, A. N. (2009). Rare earth and trace element
1479 geochemistry of termite mounds in central and northeastern Namibia: Mechanisms for micro-
1480 nutrient accumulation. *Geoderma*, *153*(1–2), 217–230.
1481 https://doi.org/10.1016/j.geoderma.2009.08.011
1482 Salonen, V.-P., & Korkka-Niemi, K. (2007). Influence of parent sediments on the concentration
1483 of heavy metals in urban and suburban soils in Turku, Finland. *Applied Geochemistry*, *22*(5),
1484 906–918. https://doi.org/10.1016/j.apgeochem.2007.02.003

1485 Sasone, F. J., Benitez-Nelson, C. R., Resing, J. A., DeCarlo, E. H., Vink, S. M., Heath, J. A.,
1486 Huebert, B. J. (2002). Geochemistry of atmospheric aerosols generated from lava-seawater
1487 interactions. *Geophysical Research Letters*, *29*(9), 49-1-49-4.
1488 https://doi.org/10.1029/2001GL013882
1489 Scanza, R. A., Mahowald, N., Ghan, S., Zender, C. S., Kok, J. F., Liu, X., Zhang, Y., & Albani,
1490 S. (2015). Modeling dust as component minerals in the Community Atmosphere Model:
1491 Development of framework and impact on radiative forcing. *Atmospheric Chemistry and*
1492 *Physics*, *15*(1). https://doi.org/10.5194/acp-15-537-2015
1493 Schlesinger, W. H., Klein, E. M., & Vengosh, A. (2017). Global biogeochemical cycle of
1494 vanadium. *Proceedings of the National Academy of Sciences of the United States of America*,
1495 *114*(52), E11092–E11100. https://doi.org/10.1073/pnas.1715500114
1496 Schmidl, C., Marr, I. L., Caseiro, A., Kotianová, P., Berner, A., Bauer, H., Kasper-Giebl, A., &
1497 Puxbaum, H. (2008). Chemical characterisation of fine particle emissions from wood stove
1498 combustion of common woods growing in mid-European Alpine regions. *Atmospheric*
1499 *Environment*, *42*(1), 126–141. https://doi.org/10.1016/j.atmosenv.2007.09.028
1500 Schutgens, N. A. J., Gryspeerdt, E., Weigum, N., Tsyro, S., Goto, D., Schulz, M., & Stier, P.
1501 (2016). Will a perfect model agree with perfect observations? The impact of spatial sampling.
1502 *Atmospheric Chemistry and Physics*, *16*(10), 6335–6353. https://doi.org/10.5194/acp-16-6335-
1503 2016
1504 Sedwick, P. N., Sholkovitz, E. R., & Church, T. M. (2007). Impact of anthropogenic combustion
1505 emissions on the fractional solubility of aerosol iron: Evidence from the Sargasso Sea.
1506 *Geochemistry, Geophysics, Geosystems*, *8*(10). https://doi.org/10.1029/2007GC001586

1507 Selin, N. E. (2009). Global biogeochemical cycling of mercury: A review. *Annual Review of*
1508 *Environment and Resources*, *34*, 43–63. https://doi.org/10.1146/annurev.environ.051308.084314
1509 Sen, I. S., & Peucker-Ehrenbrink, B. (2012). Anthropogenic Disturbance of Element Cycles at
1510 the Earth's Surface. *Environmental Science & Technology*, *46*(16), 8601–8609.
1511 https://doi.org/10.1021/es301261x
1512 Sheikh-Abdullah, S. M. (2019). Availability of Fe, Zn, Cu, and Mn in Soils of Sulaimani
1513 Governorate, Kurdistan Region, Iraq. *Soil Science*, *184*(3), 87–94.
1514 https://doi.org/10.1097/SS.0000000000000255
1515 Sheppard, S. C., Grant, C. A., & Drury, C. F. (2009). Trace elements in Ontario soils - mobility,
1516 concentration profiles, and evidence of non-point-source pollution. *Canadian Journal of Soil*
1517 *Science*, *89*(4), 489–499. https://doi.org/10.4141/cjss08033
1518 Sierra, C. A., Trumbore, S. E., Davidson, E. A., Vicca, S., & Janssens, I. (2015). Sensitivity of
1519 decomposition rates of soil organic matter with respect to simultaneous changes in temperature
1520 and moisture. *Journal of Advances in Modeling Earth Systems*, *7*(1), 335–356.
1521 https://doi.org/https://doi.org/10.1002/2014MS000358
1522 Skordas, K., Papastergios, G., & Filippidis, A. (2013). Major and trace element contents in
1523 apples from a cultivated area of central Greece. *Environmental Monitoring and Assessment*,
1524 *185*(10), 8465–8471. https://doi.org/10.1007/s10661-013-3188-1
1525 Smeltzer, G. G., Langille, W. M., & MacLean, K. S. (1962). Effects of some trace elements on
1526 grass and legume production in Nova Scotia. *Canadian Journal of Plant Science*, *42*(1), 46–52.
1527 https://doi.org/10.4141/cjps62-006

1528 Smith, R. D., Campbell, J. A., & Nielson, K. K. (1979). Characterization and formation of
1529 submicron particles in coal-fired plants. *Atmospheric Environment (1967)*, *13*(5), 607–617.
1530 https://doi.org/10.1016/0004-6981(79)90189-6
1531 Soil Survey Staff. (2011). *Soil Survey Laboratory Information Manual Soil Survey Investigations*
1532 *Report No. 45*.
1533 Spiro, P. A., Jacob, D. J., & Logan, J. A. (1992). Global inventory of sulfur emissions with 1° ×
1534 1° resolution. *Journal of Geophysical Research*, *97*(D5), 6023–6036.
1535 https://doi.org/10.1029/91JD03139
1536 Stajković-Srbinović, O., Buntić, A., Rasulić, N., Kuzmanović, Đ., Dinić, Z., Delić, D., & Mrvić,
1537 V. (2018). Microorganisms in soils with elevated heavy metal concentrations in southern Serbia.
1538 *Archives of Biological Sciences*, *70*(4), 707–716.
1539 https://www.serbiosoc.org.rs/arch/index.php/abs/article/view/2913
1540 Stankovic, D., Krstic, B., Knezevic, M., Sijacic-Nikolic, M., & Bjelanovic, I. (2012).
1541 oncentrations of heavy metals in soil in the area of the protected natural resource “Avala” in
1542 Belgrade. *Fresenius Environmental Bulletin*, *21*(2A), 495–502.
1543 Steenari, B. M., Schelander, S., & Lindqvist, O. (1999). Chemical and leaching characteristics of
1544 ash from combustion of coal, peat and wood in a 12MW CFB – a comparative study. *Fuel*,
1545 *78*(2), 249–258. https://doi.org/10.1016/S0016-2361(98)00137-9
1546 Stegemann, J. A., Roy, A., Caldwell, R. J., Schilling, P. J., & Tittsworth, R. (2000).
1547 Understanding Environmental Leachability of Electric Arc Furnace Dust. *Journal of*
1548 *Environmental Engineering*, *126*(2), 112–120. https://doi.org/10.1061/(ASCE)0733-
1549 9372(2000)126:2(112)

1550 Stehouwer, R. C., Hindman, J. M., & MacDonald, K. E. (2010). Nutrient and Trace Element
1551 Dynamics in Blended Topsoils Containing Spent Foundry Sand and Compost. *Journal of*
1552 *Environmental Quality*, *39*(2), 587–595. https://doi.org/10.2134/jeq2009.0172
1553 Steinnes, E., Lukina, N., Nikonov, V., Aamlid, D., & Røyset, O. (2000). A gradient study of 34
1554 elements in the vicinity of a copper-nickel smelter in the Kola peninsula. *Environmental*
1555 *Monitoring and Assessment*, *60*(1), 71–88. https://doi.org/10.1023/A:1006165031985
1556 Stendahl, J., Berg, B., & Lindahl, B. D. (2017). Manganese availability is negatively associated
1557 with carbon storage in northern coniferous forest humus layers. *Scientific Reports*, *7*(1).
1558 https://doi.org/10.1038/s41598-017-15801-y
1559 Sterckeman, T., Douay, F., Baize, D., Fourrier, H., Proix, N., Schwartz, C., & Carignan, J.
1560 (2006a). Trace element distributions in soils developed in loess deposits from northern France.
1561 *European Journal of Soil Science*, *57*(3), 392–410. https://doi.org/10.1111/j.1365-
1562 2389.2005.00750.x
1563 Sterckeman, T., Douay, F., Baize, D., Fourrier, H., Proix, N., & Schwartz, C. (2006b). Trace
1564 elements in soils developed in sedimentary materials from Northern France. *Geoderma*, *136*(3–
1565 4), 912–929. https://doi.org/10.1016/j.geoderma.2006.06.010
1566 Su, Y., & Yang, R. (2008). Background concentrations of elements in surface soils and their
1567 changes as affected by agriculture use in the desert-oasis ecotone in the middle of Heihe River
1568 Basin, North-west China. *Journal of Geochemical Exploration*, *98*(3), 57–64.
1569 https://doi.org/10.1016/j.gexplo.2007.12.001
1570 Trum, F., Titeux, H., Ponette, Q., & Berg, B. (2015). Influence of manganese on decomposition
1571 of common beech (Fagus sylvatica L.) leaf litter during field incubation. *Biogeochemistry*,
1572 *125*(3), 349–358. https://doi.org/10.1007/s10533-015-0129-9

1573 Tsai, S.-L., & Tsai, M.-S. (1998). A study of the extraction of vanadium and nickel in oil-fired
1574 fly ash. *Resources, Conservation and Recycling*, *22*(3–4), 163–176.
1575 https://doi.org/10.1016/S0921-3449(98)00007-X
1576 Tsikritzis, L. I., Ganatsios, S. S., Duliu, O. G., Kavouridis, C. v, & Sawidis, T. D. (2002). Trace
1577 elements distribution in soil in areas of lignite power plants of Western Macedonia. *Journal of*
1578 *Trace and Microprobe Techniques*, *20*(2), 269–282. https://doi.org/10.1081/TMA-120003729
1579 Tume, P., Bech, J., Reverter, F., Bech, J., Longan, L., Tume, L., & Sepúlveda, B. (2011).
1580 Concentration and distribution of twelve metals in Central Catalonia surface soils. *Journal of*
1581 *Geochemical Exploration*, *109*(1), 92–103.
1582 https://doi.org/https://doi.org/10.1016/j.gexplo.2010.10.013
1583 Tyler, G. (2004). Vertical distribution of major, minor, and rare elements in a Haplic Podzol.
1584 *Geoderma*, *119*(3–4), 277–290. https://doi.org/10.1016/j.geoderma.2003.08.005
1585 U.S. Geological Survey. (2022). *Mineral commodity summaries 2022*.
1586 https://doi.org/10.3133/mcs2022
1587 Vance, N. C., & Entry, J. A. (2000). Soil properties important to the restoration of a Shasta red
1588 fir barrens in the Siskiyou Mountains. *Forest Ecology and Management*, *138*(1–3), 427–434.
1589 https://doi.org/10.1016/S0378-1127(00)00428-X
1590 Vandenbussche, S., Callewaert, S., Schepanski, K., & Mazière, M. D. (2020). North African
1591 mineral dust sources: new insights from a combined analysis based on 3D dust aerosol
1592 distributions, surface winds and ancillary soil parameters. *Atmospheric Chemistry and Physics*,
1593 *20*(23), 15127-15146. https://doi.org/10.5194/acp-20-15127-2020
1594 van der Werf, G. R., Randerson, J. T., Collatz, G. J., Giglio, L., Kasibhatla, P. S., Arellano, A.
1595 F., Jr., Olson, S. C. & Kasischke, E. S. (2004). Continental-Scale Partitioning of Fire Emissions

1596 During the 1997 to 2001 El Niño/La Niña Period. *Science*, *303*, 73-76.
1597 https://10.1126/science.1090753
1598 van Diepen, L. T. A., Frey, S. D., Sthultz, C. M., Morrison, E. W., Minocha, R., Pringle, A., &
1599 Peters, D. P. C. (2015). Changes in litter quality caused by simulated nitrogen deposition
1600 reinforce the N-induced suppression of litter decay. *Ecosphere*, *6*(10).
1601 https://doi.org/10.1890/ES15-00262.1
1602 van Marle, M. J. E., Kloster, S., Magi, B. I., Marlon, J. R., Daniau, A.-L., Field, R. D., Arneth,
1603 A., Forrest, M., Hantson, S., Kehrwald, N. M., Knorr, W., Lasslop, G., Li, F., Mangeon, S., Yue,
1604 C., Kaiser, J. W., & van der Werf, G. R. (2017). Historic global biomass burning emissions for
1605 CMIP6 (BB4CMIP) based on merging satellite observations with proxies and fire models (1750–
1606 2015). *Geoscientific Model Development*, *10*(9), 3329–3357. https://doi.org/10.5194/gmd-10-
1607 3329-2017
1608 Vejnovic, J., Djuric, B., Lombnæs, P., & Singh, B. R. (2018). Concentration of trace and major
1609 elements in natural grasslands of Bosnia and Herzegovina in relation to soil properties and plant
1610 species. *Acta Agriculturae Scandinavica, Section B — Soil & Plant Science*, *68*(3), 243–254.
1611 https://doi.org/10.1080/09064710.2017.1388439
1612 Voutsa, D., & Samara, C. (2002). Labile and bioaccessible fractions of heavy metals in the
1613 airborne particulate matter from urban and industrial areas. *Atmospheric Environment*, *36*(22),
1614 3583-3590.
1615 Wang, Z., Wade, A. M., Richter, D. D., Stapleton, H. M., Kaste, J. M., & Vengosh, A. (2022).
1616 Legacy of anthropogenic lead in urban soils: Co-occurrence with metal(loids) and fallout
1617 radionuclides, isotopic fingerprinting, and in vitro bioaccessibility. *Science of The Total*
1618 *Environment*, *806*, 151276. https://doi.org/10.1016/j.scitotenv.2021.151276

1619 Watson, J. G., Chow, J. C., & Houck, J. E. (2001). PM2.5 chemical source profiles for vehicle
1620 exhaust, vegetative burning, geological material, and coal burning in Northwestern Colorado
1621 during 1995. *Chemosphere*, *43*(8), 1141–1151. https://doi.org/10.1016/S0045-6535(00)00171-5
1622 Webb, N. P., & Pierre, C. (2018). Quantifying Anthropogenic Dust Emissions. *Earth's Future*,
1623 *6*(2), 286–295. https://doi.org/10.1002/2017EF000766
1624 Wen, B., Li, L., Duan, Y., Zhang, Y., Shen, J., Xia, M., Wang, Y., Fang, W., & Zhu, X. (2018).
1625 Zn, Ni, Mn, Cr, Pb and Cu in soil-tea ecosystem: The concentrations, spatial relationship and
1626 potential control. *Chemosphere*, *204*, 92–100.
1627 https://doi.org/https://doi.org/10.1016/j.chemosphere.2018.04.026
1628 Whalen, E. D., Smith, R. G., Grandy, A. S., & Frey, S. D. (2018). Manganese limitation as a
1629 mechanism for reduced decomposition in soils under atmospheric nitrogen deposition. *Soil*
1630 *Biology and Biochemistry*, *127*, 252–263. https://doi.org/10.1016/j.soilbio.2018.09.025
1631 Wieder, W.R., Boehnert J., Bonan G. B., & Langseth M. (2014). Regridded Harmonized World
1632 Soil Database v1.2. Data set. Available on-line [http://daac.ornl.gov] from Oak Ridge National
1633 Laboratory Distributed Active Archive Center, Oak Ridge, Tennessee, USA.
1634 http://dx.doi.org/10.3334/ORNLDAAC/1247 .
1635 Wiedinmyer, C., Lihavainen, H., Mahowald, N., Alastuey, A., Albani, S., Artaxo, P., Bergametti,
1636 G., Batterman, S., Brahney, J., Duce, R., Feng, Y., Buck, C., Ginoux, P., Chen, Y., Guieu, C.,
1637 Cohen, D., Hand, J., Harrison, R., Herut, B., . . . & Zhang, Y. (2018). *COARSEMAP: synthesis of*
1638 *observations and models for coarse-mode aerosols*. AGU Fall Meeting New-Orleans, 2017.
1639 Wilcke, W., Krauss, M., & Kobza, J. (2005). Concentrations and forms of heavy metals in
1640 Slovak soils. *Journal of Plant Nutrition and Soil Science*, *168*(5), 676–686.
1641 https://doi.org/10.1002/jpln.200521811

1642 Wong, M. Y., Rathod, S. D., Marino, R., Li, L., Howarth, R. W., Alastuey, A., Alaimo, M. G.,
1643 Barraza, F., Carneiro, M. C., Chellam, S., Chen, Y. C., Cohen, D. D., Connelly, D., Dongarra,
1644 G., Gómez, D., Hand, J., Harrison, R. M., Hopke, P. K., Hueglin, C., … Mahowald, N. M.
1645 (2021). Anthropogenic Perturbations to the Atmospheric Molybdenum Cycle. *Global*
1646 *Biogeochemical Cycles*, *35*(2). https://doi.org/10.1029/2020GB006787
1647 Woo, D. K., & Seo, Y. (2022). Effects of elevated temperature and abnormal precipitation on
1648 soil carbon and nitrogen dynamics in a Pinus densiflora forest. *Frontiers in Forests and Global*
1649 *Change*, *5*. https://doi.org/10.3389/ffgc.2022.1051210
1650 Xianmo, Z., Yushan, L., Xianglin, P., & Shuguang, Z. (1983). Soils of the loess region in China.
1651 *Geoderma*, *29*(3), 237–255. https://doi.org/https://doi.org/10.1016/0016-7061(83)90090-3
1652 Yalcin, M. G., Battaloglu, R., & Ilhan, S. (2007). Heavy metal sources in sultan marsh and its
1653 neighborhood, kayseri, turkey. *Environmental Geology*, *53*(2), 399–415.
1654 https://doi.org/10.1007/s00254-007-0655-4
1655 Yang, C., Guo, R., Liu, R., Yue, Q., Ren, X., & Wu, Z. (2012). PCA analysis and Concentration
1656 of Heavy Metal in the Soil, Guangdong, China. *Advanced Materials Research*, *518-523*, 1952-
1657 1955. https://doi.org/10.4028/www.scientific.net/AMR.518-523.1952
1658 Yang, S., Zhou, D., Yu, H., Wei, R., & Pan, B. (2013). Distribution and speciation of metals (Cu,
1659 Zn, Cd, and Pb) in agricultural and non-agricultural soils near a stream upriver from the Pearl
1660 River, China. *Environmental Pollution*, *177*, 64–70.
1661 https://doi.org/https://doi.org/10.1016/j.envpol.2013.01.044
1662 Yilmaz, F., Yilmaz, Y. Z., Ergin, M., Erkol, A. Y., Muftuoglu, A. E., & Karakelle, B. (2003).
1663 Heavy metal concentrations in surface soils of Izmit Gulf region, Turkey. *Journal of Trace and*
1664 *Microprobe Techniques*, *21*(3), 523–531. https://doi.org/10.1081/TMA-120023068

1665 Yu, C., Cheng, J. J., Jones, L. G., Wang, Y. Y., Faillace, E., Loureiro, C., & Chia, Y. P. (1993).
1666 *Data collection handbook to support modeling the impacts of radioactive material in soil*. United
1667 States. https://doi.org/10.2172/10162250
1668 Yu, C., Peng, B., Peltola, P., Tang, X., & Xie, S. (2012). Effect of weathering on abundance and
1669 release of potentially toxic elements in soils developed on Lower Cambrian black shales, P. R.
1670 China. *Environmental Geochemistry and Health*, *34*(3), 375–390.
1671 https://doi.org/10.1007/s10653-011-9398-y
1672 Yu, H., Chin, M., Yuan, T., Bian, H., Remer, L. A., Prospero, J. M., Omar, A., Winker, D.,
1673 Yang, Y., Zhang, Y., Zhang, Z., & Zhao, C. (2015). The fertilizing role of African dust in the
1674 Amazon rainforest: A first multiyear assessment based on data from Cloud-Aerosol Lidar and
1675 Infrared Pathfinder Satellite Observations. *Geophysical Research Letters*, *42*(6), 1984–1991.
1676 https://doi.org/10.1002/2015GL063040
1677 Zak, D. R., Freedman, Z. B., Upchurch, R. A., Steffens, M., & Kögel-Knabner, I. (2017).
1678 Anthropogenic N deposition increases soil organic matter accumulation without altering its
1679 biochemical composition. *Global Change Biology*, *23*(2), 933–944.
1680 https://doi.org/10.1111/gcb.13480
1681 Zender, C. S., Bian, H., & Newman, D. (2003). Mineral Dust Entrainment and Deposition
1682 (DEAD) model: Description and 1990s dust climatology. *Journal of Geophysical Research*
1683 *Atmospheres*, *108*(D14). https://doi.org/10.1029/2002JD002775
1684 Zhang, H., Wang, S., Hao, J., Wan, L., Jiang, J., Zhang, M., Mestl, H. E. S., Alnes, L. W. H.,
1685 Aunan, K., & Mellouki, A. W. (2012). Chemical and size characterization of particles emitted
1686 from the burning of coal and wood in rural households in Guizhou, China. *Atmospheric*
1687 *Environment*, *51*, 94–99. https://doi.org/10.1016/j.atmosenv.2012.01.042

1688 Zhang, L., Zheng, Q., Liu, Y., Liu, S., Yu, D., Shi, X., Xing, S., Chen, H., & Fan, X. (2019).
1689 Combined effects of temperature and precipitation on soil organic carbon changes in the uplands
1690 of eastern China. *Geoderma*, *337*, 1105–1115.
1691 https://doi.org/https://doi.org/10.1016/j.geoderma.2018.11.026
1692 Zhang, X.-Y., Tang, L.-S., Zhang, G., & Wu, H.-D. (2009). Heavy Metal Contamination in a
1693 Typical Mining Town of a Minority and Mountain Area, South China. *Bulletin of Environmental*
1694 *Contamination and Toxicology*, *82*(1), 31–38. https://doi.org/10.1007/s00128-008-9569-4
1695 Zhao, B., Zhuang, Q., Shurpali, N., Köster, K., Berninger, F., & Pumpanen, J. (2021a). North
1696 American boreal forests are a large carbon source due to wildfires from 1986 to 2016. *Scientific*
1697 *Reports*, *11*(1). https://doi.org/10.1038/s41598-021-87343-3
1698 Zhao, F., Wu, Y., Hui, J., Sivakumar, B., Meng, X., & Liu, S. (2021b). Projected soil organic
1699 carbon loss in response to climate warming and soil water content in a loess watershed. *Carbon*
1700 *Balance and Management*, *16*(1), 24. https://doi.org/10.1186/s13021-021-00187-2
1701 Zorer, Ö., Ceylan, H., & Doğru, M. (2009). Determination of heavy metals and comparison to
1702 gross radioactivity concentration in soil and sediment samples of the Bendimahi River Basin
1703 (Van, Turkey). Water, Air, & Soil Pollution, 196(1–4), 75–87. https://doi.org/10.1007/s11270-
1704 008-9758-0